Benthic Foraminifera in Arctic Methane Hydrate Bearing Sediments

Pierre-Antoine Dessandier[1]*, Chiara Borrelli[2], Dimitri Kalenitchenko[1] and Giuliana Panieri[1]

[1] Centre for Arctic Gas Hydrate, Environment and Climate, Department of Geosciences, UiT The Arctic University of Norway, Tromsø, Norway, [2] Department of Earth and Environmental Sciences, University of Rochester, Rochester, NY, United States

Benthic foraminifera have been widely used as proxy for paleo-methane emissions, mainly based on their stable isotopic signature. In cold seeps, the ecology of these organisms remains uncertain, in particular their ability to thrive during active phases of seepage. In this study, we evaluate the benthic foraminiferal response to methane seepage in Arctic sediments. We do so by examining living and dead benthic foraminiferal assemblages (>63 µm) of 11 push cores collected in two of the most active pockmarks (Lunde and Lomvi) along Vestnesa Ridge, offshore western Svalbard. Benthic foraminiferal assemblages are interpreted in the context of sediment geochemistry, seafloor images, and pore water analyses, which are used to characterize the different microhabitats. At the sampling locations, methane is currently being released making these the ideal sites to investigate the connection between the benthic foraminiferal distribution and methane seepage in the Arctic Ocean. Our results show that benthic calcareous foraminifera live in methane charged sediments, even if the faunal density and diversity is low. We note that the eutrophic-tolerant species *Melonis barleeanus* withstand the methane-induced hostile geochemical conditions and that it seems to prosper on the additional food availability represented by microbial mats growing at methane seeps. We also observe that the methane transport mechanisms affect different species differently. For example, sediments characterized by advective-like conditions are distinguished by a high density of living individuals, dominated by *Cassidulina neoteretis*, whereas sediments characterized by methane diffusion exhibit a very low faunal density. Agglutinated foraminifera are less abundant in sediments influenced by methane seepage, suggesting that this group of foraminifera does not tolerate the geochemical conditions at seeps. A comparison between the size fractions >63 and >125 µm highlights the importance of studying the finer size fraction for ecological studies in the Arctic Ocean. In the light of our results, we conclude that benthic foraminiferal can thrive at active methane seeps, where assemblages are clearly affected by methane flux.

Keywords: benthic foraminiferal assemblages, methane advection, methane diffusion, Arctic Ocean, microbial mats

INTRODUCTION

The Arctic Ocean is a fundamental component of the climate system because of its role in the global carbon dioxide (CO_2) and methane (CH_4) cycles (e.g., McGuire et al., 2009). It represents a very large CH_4 reservoir stored in terrestrial and marine permafrost and gas hydrates, which are sensitive to temperature changes (Corell et al., 2008) and is one of the most sensitive areas affected by the current climate change (e.g., Screen and Simmonds, 2010; Serreze and Barry, 2011; Ipcc, 2013). On western Svalbard, multiple seepage episodes were linked with faults reactivation and fracturing over the last 2.7 Ma (Plaza-Faverola et al., 2015) and, for the post-LGM, seepages were induced by fault and fracture reopening caused by glacioisostatic adjustment of Svalbard (Schneider et al., 2018). Recent modeling simulations showed that Western Svalbard cold-seep system has been actively releasing methane for the last 6 Ma, charging the seafloor with migrating hydrocarbons over the last 2 Ma (Knies et al., 2018). In this area, the Vestnesa Ridge hosts a gas hydrate system with associate gas seepages (Vogt et al., 1994; Hustoft et al., 2009; Petersen et al., 2010; Bünz et al., 2012; Panieri et al., 2017). Previous investigation at Vestnesa Ridge revealed that the methane been released from small depressing termed pits within two active pockmarks called Lunde and Lomvi (Bünz et al., 2012) is a mixture of microbial and thermogenic methane (Panieri et al., 2017).

Benthic foraminifera are eukaryotic, single-cell organisms mainly living in marine environments (Murray, 2006). These organisms primarily feed on phytodetritus (Heeger, 1990) and prokaryotes (Goldstein and Corliss, 1994), but can also ingest metazoan tissues (Linke et al., 1995). Because of this, it was proposed that aerobic methanotrophic bacteria could represent an additional food source for these organisms (e.g., Rathburn et al., 2003; Panieri, 2006; Bernhard et al., 2010), allowing them to inhabit cold seeps.

Several studies have been conducted to investigate the assemblages, and stable isotope composition, of benthic foraminifera sampled at methane seeps from different geographic locations, like the Barents Sea (Wollenburg and Mackensen, 2009); western offshore Svalbard (Panieri et al., 2016; Consolaro et al., 2018), Mediterranean Sea (Panieri, 2006), California Margin (Rathburn et al., 2000, 2003; Bernhard et al., 2001), Gulf of Mexico (Sen Gupta et al., 1997, 2007; Panieri and Sen Gupta, 2008), offshore New Zealand (Martin et al., 2010), and Niger (Fontanier et al., 2014). All these studies concluded that there are no endemic species at cold seeps, even if a lower abundance and diversity of agglutinated species was reported from sites characterized by a high methane concentration (Heinz et al., 2005; Panieri and Sen Gupta, 2008; Martin et al., 2010). In cold seep environments, a potential association of certain species with bacteria was suggested as a factor for benthic foraminiferal survival, such as *Uvigerina peregrina* in Monterey Bay (Bernhard et al., 2001) and *Melonis barleeanus* in Vestnesa Ridge (Bernhard and Panieri, 2018). Even so, the ability of benthic foraminifera to thrive during methane release remained debated (e.g., Torres et al., 2003; Herguera et al., 2014). In addition, it was demonstrated that the stable isotopic composition of benthic
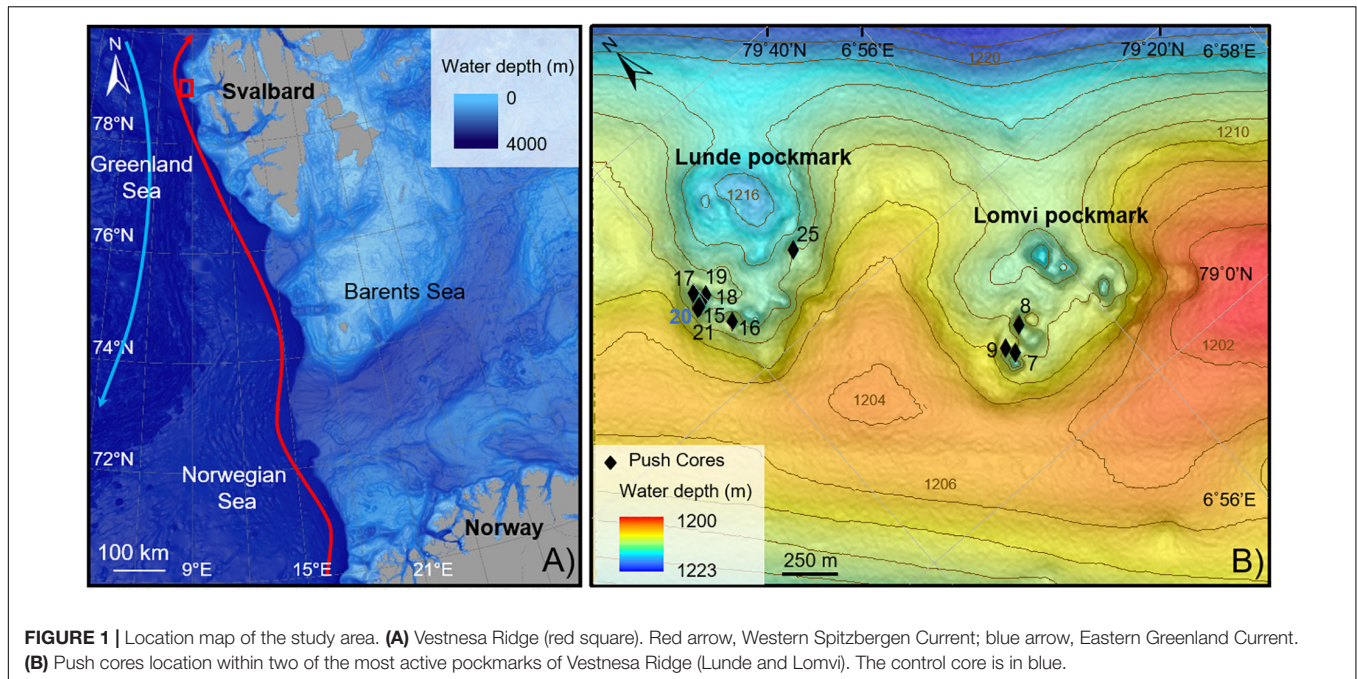
foraminifera from cold seeps can be significantly affected by the precipitation of methane-derived authigenic carbonate (MDAC), as highlighted by studies conducted on foraminifera from Vestnesa Ridge (Panieri et al., 2014, 2017; Consolaro et al., 2015; Schneider et al., 2017; Dessandier et al., under review). Therefore, a good knowledge of species ecology could provide additional information to better understand how benthic foraminifera can live and record methane seepage episodes.

In this study, we investigate the influence of methane seepage on the benthic foraminiferal assemblages at gas hydrate-bearing sediments in the Arctic Ocean. We present a unique and comprehensive dataset on living (Rose Bengal stained) and dead benthic foraminifera (fraction > 63 μm) from 11 push cores collected in the two pockmarks Lunde and Lomvi. Methane is currently being released at these locations, making them the ideal sites to investigate the connection between the benthic foraminiferal distribution and methane seepage in the Arctic Ocean. Combining the foraminiferal data with sediment analyses (total organic carbon, $\delta^{13}C_{TOC}$), we assess the influence of potential stress factors, like a chemical hostile environment and/or impact of the microbiological activity on the benthic foraminiferal assemblages inhabiting Arctic methane seeps. Finally, we evaluate the impact of the size fraction analyzed on benthic foraminiferal studies, demonstrating that key species for oceanographic investigations in the Arctic Ocean can be significantly over- or under-estimated when only the coarser fraction is considered.

STUDY AREA

The eastern Fram Strait is climatically very sensitive, under the influence of two major currents: the warm and saline North Atlantic Current (NAC), via its local branch West Spitzbergen current (WSC), flowing northward (red arrow, **Figure 1A**) and the polar East Greenland Current (EGC, Aagaard et al., 1987) flowing southward (blue arrow, **Figure 1A**). Both these currents act on the northern hemisphere climate (Overpeck et al., 1997).

The Fram Strait is characterized by the northern extension of the Mid-Atlantic Ridge system, associated with several transform faults, connecting the Knipovich Ridge with the Gakkel Ridge in the Arctic. The Molloy transform fault, abutting the West-Svalbard margin at 79°N, bends the Vestnesa Ridge SE-NW to E-W, a 100 km-long sediment drift at 1200 m water depth (Talwani and Eldholm, 1977; Thiede et al., 1998; Bünz et al., 2012). The West-Svalbard margin is a young (<20 Ma) oceanic crust covered by a ~2 km thick sediment layer from glaciomarine and hemipelagic origin (Eiken and Hinz, 1993; Hustoft et al., 2009). The Vestnesa Ridge grows due to bottom-current controlled sediment dynamics and is also influenced by the WSC, shaping the morphology of the Ridge (Eiken and Hinz, 1993). Erosion or non-deposition throughout the Holocene expose sediments older than 10–9 ka at the seafloor (Elverhøi et al., 1995; Howe et al., 2008; Schneider et al., 2018). These muddy-silty contourites surface sediments cover a period until the early Holocene, showing abundant ice rafted debris and a sedimentation rate of about 10 cm kyrs^{-1} (Howe et al., 2008).

FIGURE 1 | Location map of the study area. **(A)** Vestnesa Ridge (red square). Red arrow, Western Spitzbergen Current; blue arrow, Eastern Greenland Current. **(B)** Push cores location within two of the most active pockmarks of Vestnesa Ridge (Lunde and Lomvi). The control core is in blue.

Consolaro et al. (2015) estimated sedimentation rates during the deglaciation of ∼40–50 cm kyrs^{-1} and a current sedimentation rate of ∼19 cm kyrs^{-1}.

The crest of the Vestnesa Ridge presents a 50 km-long belt of pockmarks, which vary in size and can be up to 700 m diameter and 10 m deep (Vogt et al., 1994; Bünz et al., 2012). Pockmarks are assumed to be caused by the eruption of gas and seepage of gas and pore fluids in soft grained-sediments (Judd and Hovland, 2007). Some of these pockmarks are active, releasing methane-rich fluids from confined deep water gas hydrate and free gas reservoirs into the water column, as observed in gas flares up to 900 m high (Bünz et al., 2012; Smith et al., 2014). Geochemical analyses of gas hydrates collected from Vestnesa pockmarks revealed a thermogenic origin of the methane trapped (Smith et al., 2014). At Vestnesa Ridge, the two most active pockmarks are called Lunde and Lomvi (**Figure 1B**). Both pockmarks display authigenic carbonates and patches of chemosynthetic communities related to biogenic and thermogenic methane release at the seafloor (Panieri et al., 2017).

MATERIALS AND METHODS

Samples Collection

Push cores were collected using the remotely operated vehicle (ROV, "AEgir 6000") during the cruise P1606 (July 15–16, 2016) on board the R/V G.O. Sars. The cores were collected within two active pockmarks (Lunde and Lomvi; **Figure 1B**). In particular, eight push cores were retrieved from the Lunde pockmark (cores 15, 16, 17, 18, 19, 20, 21, and 25) and three push cores were retrieved from the Lomvi pockmark (cores 7, 8, and 9) (**Table 1**). All cores (with the exception of core 20) were obtained from areas covered by bacterial mats (**Figure 2A**), indicative of

chemosynthetic communities and methane seepage. Core 20 was collected in sediment devoid of any chemosynthetic community (**Figure 2A**). Because of this, and considering core 20 pore water data (Yao et al., 2019), we considered this core our control core (core not influenced by methane seepage).

Geochemical Analyses

The surface sediment (0–1 cm) of all push cores, including the microbial mat when present, was subsampled for organic matter analyses. Total organic carbon (TOC) and organic matter carbon stable isotopes ($\delta^{13}C_{TOC}$) were measured on freeze-dried sediment after acid treatment (HCl 6M for 48 h at room temperature) to remove carbonates. Samples were washed in deionized water and dried at 50°C (24 h). After pulverizing the samples in a mortar, they were placed into Sn-capsules, weighted, and combusted in an Elemental Analyzer (Thermo Scientific Flash HT Plus) at 1020°C, before being analyzed with an Isotope Ratio Mass Spectrometer (Thermo Scientific MAT253) at UiT, the Arctic University of Norway in Tromsø. $\delta^{13}C_{TOC}$ was determined by normalization to international scales VPDB (Vienna Pee Dee Belemnite), by three in-house standards with isotopic values that enclose the isotopic values of the samples. The in-house standards were previously normalized by using several international standards. The instrument uncertainty for $\delta^{13}C$ of perfectly homogenous material is ≤0.15 ‰ (1 standard deviation; Thermo Scientific). For the estimate of the sulfate-methane transition zone and the dissolved inorganic carbon $\delta^{13}C$ (**Table 1**), we referred to Dessandier et al. (under review).
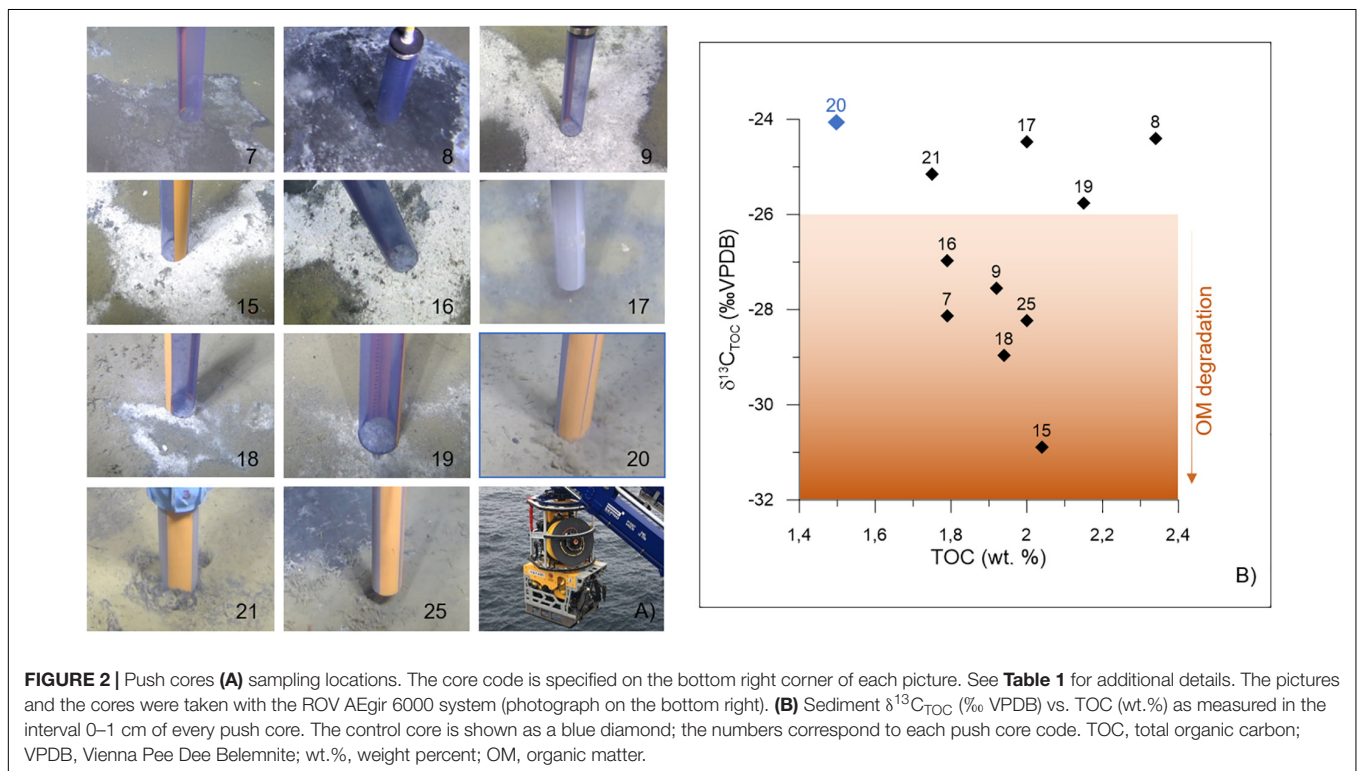
Benthic Foraminiferal Analyses

Push core 8 from Lomvi, and push cores 15, 16, 18, 19, 20, and 25 from Lunde were sliced every centimeter on board. The first 5 cm were stored in a 2 g L^{-1} Rose Bengal solution in ethanol 96%,

TABLE 1 | Coordinates and geochemistry (TOC, $\delta^{13}C_{TOC}$, $\delta^{13}C_{DIC}$ measured at 0–1 cm) of the push cores used in this study.

Push core name	Code	Pockmark	Latitude °N	Longitude °E	Water depth (m)	TOC (wt.%)	$\delta^{13}C_{TOC}$ ‰ VPDB	$\delta^{13}C_{DIC}$ ‰ VPDB	SMTZ (cmbsf)
P1606-007	7	Lomvi	79.0023	6.225	1204.0	1.79	−28.13	−30.5	10
P1606-008	8	Lomvi	79.0027	6.9248	1208.0	2.34	−24.4	−37.7	7
P1606-009	9	Lomvi	79.0025	6.922	1205.1	1.92	−27.55	−25.1	2.5
P1606-015	15	Lunde	79.0076	6.9003	1208.1	2.04	−30.89	n.d.	n.d.
P1606-016	16	Lunde	79.0068	6.9006	1205.5	1.79	−26.97	−32.6	2.5
P1606-017	17	Lunde	79.0078	6.8994	1205.0	2	−24.47	−33.8	12.5
P1606-018	18	Lunde	79.0075	6.899	1207.2	1.94	−28.96	−39.4	n.d.
P1606-019	19	Lunde	79.0075	6.8986	1206.6	2.15	−25.76	n.d.	n.d.
P1606-020	**20**	**Lunde**	**79.0075**	6.899	**1206.7**	1.5	−24.07	−1.7	Absent
P1606-021	21	Lunde	79.0075	6.8989	1206.5	1.75	−25.15	−22.4	17.5
P1606-025	25	Lunde	79.0071	6.9111	1200.0	2	−28.23	n.d.	12.5

The control core is identified by bold characters. In the main text, the cores are identified by their code for practical purposes. TOC, total organic carbon; SMTZ, sulfate-methane transition zone; DIC, dissolved inorganic carbon.

FIGURE 2 | Push cores **(A)** sampling locations. The core code is specified on the bottom right corner of each picture. See **Table 1** for additional details. The pictures and the cores were taken with the ROV AEgir 6000 system (photograph on the bottom right). **(B)** Sediment $\delta^{13}C_{TOC}$ (‰ VPDB) vs. TOC (wt.%) as measured in the interval 0–1 cm of every push core. The control core is shown as a blue diamond; the numbers correspond to each push core code. TOC, total organic carbon; VPDB, Vienna Pee Dee Belemnite; wt.%, weight percent; OM, organic matter.

in order to identify the living (Walton, 1952), or recently alive (Corliss, 1991), individuals (Rose Bengal stained foraminifera) from the dead ones (non-Rose Bengal stained foraminifera). Samples were stored at 4°C for more than 14 days in the solution, following the FOBIMO protocol (Schönfeld et al., 2012). For core 20 (control core), only the first cm was available for benthic foraminiferal analyses. Because of this, all our comparisons involving living foraminifera are limited to the most superficial samples (0–1 cm). Push cores 7 and 9 from Lomvi, and 17 and 21 from Lunde were not sliced on board. Instead, they were kept frozen and sampled down to 4 cm sediment depth later in our laboratory. For this reason, these cores were not used to study the living foraminiferal assemblage.

All samples were wet sieved using 63 and 125 μm mesh sieves and dried at 40°C (48 h). Identification of living and dead individuals was determined using a stereoscopic microscope. We considered "living" individuals the ones characterized by a pink stain of all the test chambers, with the exception of the last one. In case of doubt, the test was broken to investigate the staining of the endoplasm (Schönfeld et al., 2012). All benthic foraminiferal specimens from the 63 and 125 μm size fractions were handpicked and counted. Some of the samples presented a large amount of sediment. In these cases, samples were split using an Otto microsplitter.

Faunal densities were calculated as number of individuals per 1 cm sediment layer. In those cases when sediment samples

were split, the number of individuals was multiplied by the split value. The distribution of fauna is investigated by examining the species contributing for at least 5% to the assemblage. Species that represented less than 5% were grouped together in the category "others." Diversity indices such as specific richness (S), Shannon index (H′), and Evenness index (E) were calculated on the raw data using the PAST software (Hammer et al., 2001). For faunal densities and comparison between living and dead assemblages, the 63–125 μm and >125 μm size fractions were summed up before calculating the species relative contribution. Foraminiferal raw data are available in **Supplementary Table S1**.

RESULTS

Sediment Total Organic Carbon and Organic Matter δ^{13}C

Sediment TOC and $\delta^{13}C_{TOC}$ were measured on the surface samples (0–1 cm) of all the cores available for this study. TOC values ranged from 1.50% (control core 20) to 2.34% (core 8 from Lomvi), whereas the $\delta^{13}C_{TOC}$ was comprised between −24.07‰ (control core 20) and −30.89‰ (core 15 from Lunde, **Table 1**). TOC and $\delta^{13}C_{TOC}$ values were plotted together (**Figure 2B**) to illustrate the environmental conditions at the different sampling sites.

Benthic Foraminiferal Assemblages

Benthic foraminiferal living and dead assemblages were studied in terms of diversity and faunal distribution. All faunal raw data are provided in Appendix A. Data relative to the interval 0–1 cm are shown in **Figure 3**. Very low numbers of individuals were found in the Lunde cores 15, 16, 18, and 25. In particular, we noted that the number of living foraminifera was scarce reaching 6, 6, 7, and 2 specimens in cores 15, 16, 18, and 25, respectively. These stations also displayed low diversities, with Shannon values close to 1 and number of taxa lower than 5. On the contrary, a high diversity was observed at the Lunde and Lomvi stations 8, 19 and control core 20 in both living and dead communities, with Shannon values close to 2. Significant numbers of living individuals were found in cores 8 and 19, in which *Buccella frigida* contributed to 29 and 31%, respectively, of the total assemblage. Together, *Cassidulina neoteretis* and *Cassidulina reniforme* represented 50% of the assemblage in core 8 and 23% in core 19. These numbers increased for the dead assemblages, where *Cassidulina* spp. reached 51 and 42% in cores 8 and 19, respectively, mainly due to a larger proportion of *C. reniforme*. *M. barleeanus* was not very abundant in the living assemblage of cores 8 and 19 (<8%), but it showed higher percentages in the dead assemblage reaching 17 and 21% in cores 8 and 19, respectively. Interestingly, *M. barleeanus* was the most abundant species of the dead assemblage in other cores, as well, such as cores 15 (30%), 16 (42%), 18 (41%), and 25 (33%).

The highest number of individuals was found in the control core 20 (**Figure 3B**; core 20 is highlighted by a blue square), with 219 living and 796 dead specimens. Core 20 was also characterized by the highest faunal diversity. The highest proportion of agglutinated species was found among the living

(30%) and dead (12.5%) foraminifera of this core compared to the other cores collected at sites covered by microbial mats.

The vertical faunal density of dead benthic foraminifera in all push cores (including those where living faunal data is not available) as function of sediment depth is shown in **Figure 4**. In a significant number of cores, the faunal density was lower in the surface sample (cores 7, 9, 15, 16, 17, 18, and 25), regardless the dry mass of sediment analyzed (with the exception of core 7) (**Table 2**). In this context, the low faunal density in surface samples did not reflect a sampling effect. In general, the number of individuals varied with sediment depth, but it remained roughly stable in cores 17 and 18. Cores 8, 19, and 21 showed a higher faunal number at the surface sediment (0–1 cm), and the density decreased with sediment depth in cores 8 and 19. Most of the cores showed a comparative number of individuals, except cores 16 and 21, in which we found maxima of 2790 and 1848 individuals, respectively.

Size Fraction Comparison

A comparison of the size fractions 63–125 μm and >125 μm was done on 0–5 cm sediment depth (0–2 cm for core 15) in order to investigate the influence of the size fraction on faunal distribution (**Figure 5**). Our data revealed that the number of individuals is higher in the 63–125 μm size fraction in most cores (except for cores 7, 15, and 16) (**Figure 5A**). On average, 63% of all individuals examined in this study came from the finer fraction.

In terms of species distribution, *B. frigida*, *C. reniforme*, and *M. barleeanus* were the only species, among the major ones (>5%), showing large variability (>10%) between 63–125 μm and >125 μm size fractions. Specifically, *M. barleeanus* was the dominant species in the coarse fraction, whereas *B. frigida* and *C. reniforme* showed relatively higher percentages in the finer fraction (**Figure 5B**). *B. frigida* showed relative contributions from 4 to 17% in the 63–125 μm and from 2 to 15% in the >125 μm size fraction. At all sampling sites, *C. reniforme* was most abundant in the finer fraction (12–32%) compared to the coarser one (1–6%). On the contrary, *M. barleeanus* showed often higher relative contributions (3–52%) in the coarse fraction than in 63–125 μm (13–32%) as it was the case in all cores from the Lunde pockmark except core 25, which was highly dominated by *C. neoteretis*. In the cores from the Lomvi pockmark (7, 8, and 9), the abundance of *M. barleeanus* was similar in both size fractions (∼20%). These differences were also visible in faunal diversity, with higher specific richness and Shannon index in the finer size fraction in cores 8, 15, 17, 18, 19, and 21 (**Figure 5B**). Evenness (E) values did not show any specific trend between the two size fractions, except for core 8 with much higher E for the coarse size fraction. Cores 25 and 18 showed the highest E values (>0.8) in both size fractions. The most common species from the two size fractions are presented in **Figure 6**.

DISCUSSION

Methane-Related Habitat Conditions

The diverse environmental conditions in marine sediments are usually determined using geochemical proxies, such as
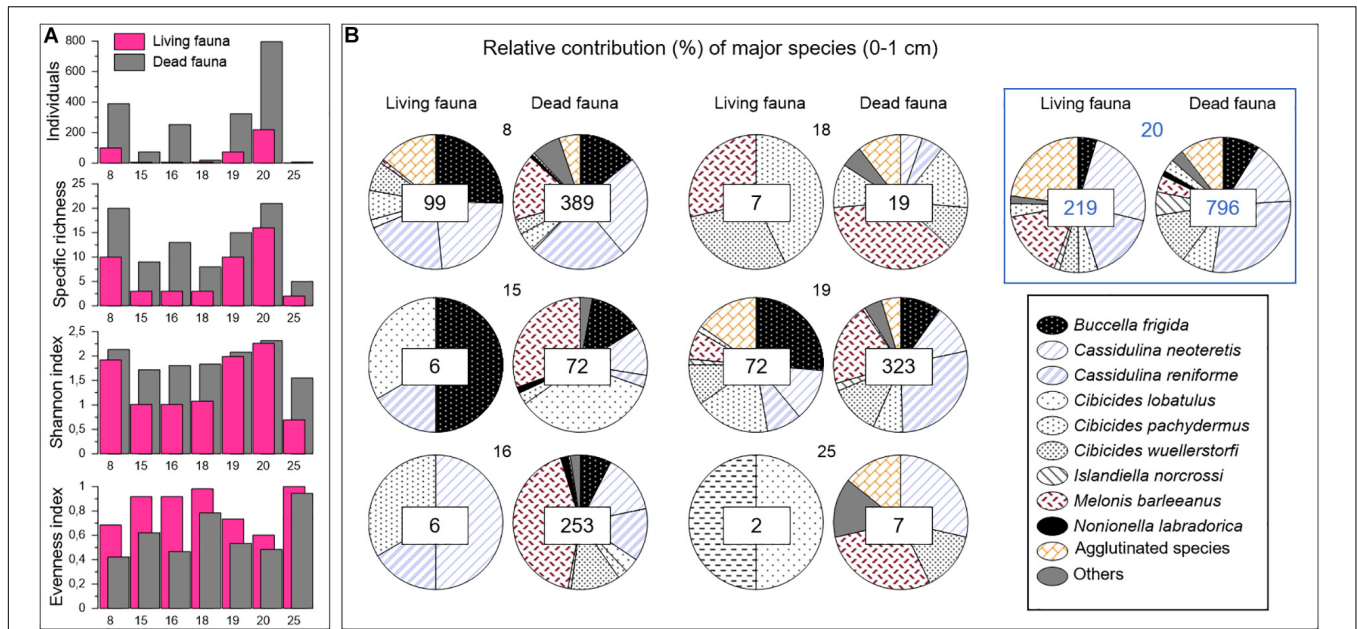
FIGURE 3 | Surface sample (0–1 cm) faunal data from the summed 63–125 μm and >125 μm size fractions. **(A)** Number of individuals and diversity indices of living and dead faunas. **(B)** Relative contribution of major species in living and dead assemblages. The number of individuals considered to build the relative contribution are specified in squares at the center of the diagrams. Push core codes are indicated on the top of the plots. The control core is identified by the blue square.
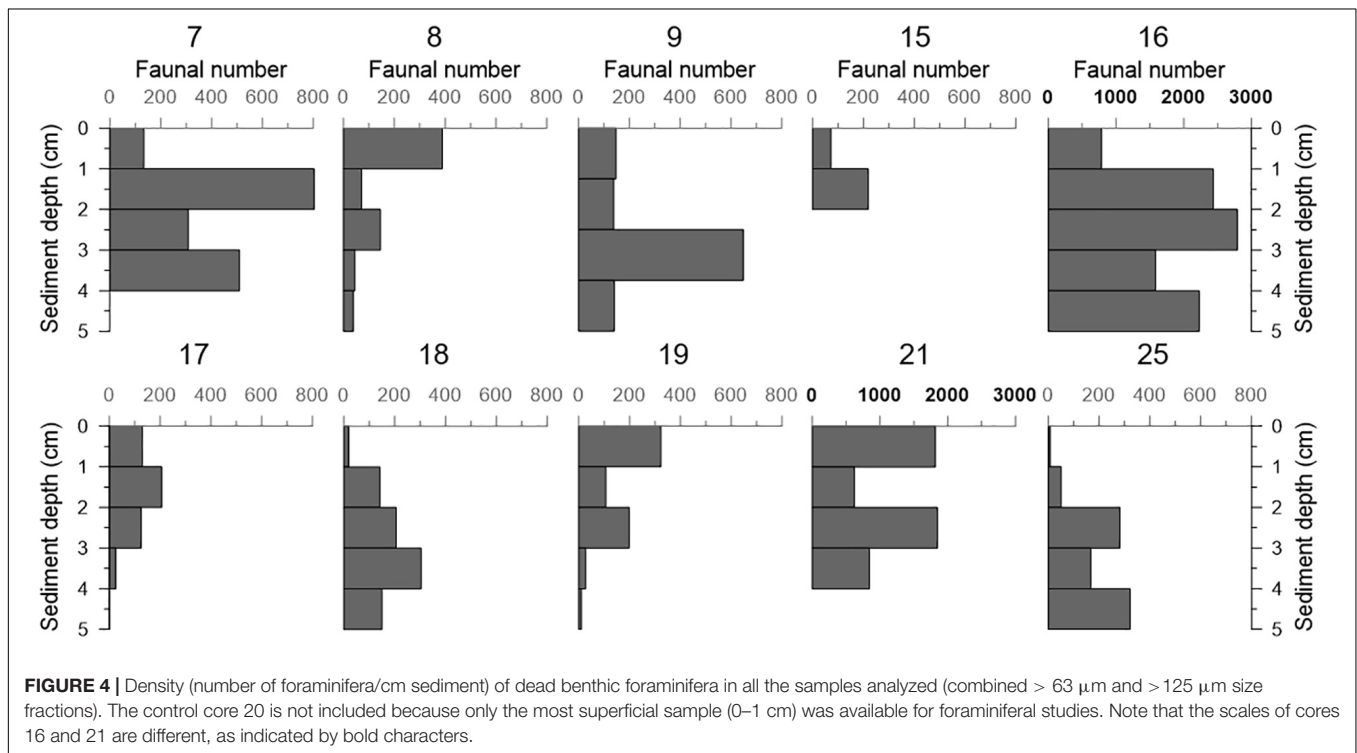
FIGURE 4 | Density (number of foraminifera/cm sediment) of dead benthic foraminifera in all the samples analyzed (combined > 63 μm and >125 μm size fractions). The control core 20 is not included because only the most superficial sample (0–1 cm) was available for foraminiferal studies. Note that the scales of cores 16 and 21 are different, as indicated by bold characters.

TOC to quantify the amount of organic matter in sediments, or $\delta^{13}C_{TOC}$ to evaluate the TOC source (Gordon and Goñi, 2003). The analysis of these proxies on surface (0–1 cm) sediment samples of the push cores used in this study showed a higher organic content (1.7–2.4%) in all the sampling sites,

with the exception of core 20 (**Figure 2B**), compared to what is commonly observed in Arctic environments (~1% in average, Knies and Martinez, 2009). The high TOC values in cores sampled on microbial mats can be explained by the presence of microbes, which are a source of carbon in

the form of microbial extracellular polymeric substance (EPS) (Decho and Gutierrez, 2017).

The $\delta^{13}C_{TOC}$ is a classical proxy to study the nature and source of organic matter, in particular because the isotopic signature remains intact for million-year periods despite early diagenesis (Meyers, 1994). At Vestnesa Ridge, the source of organic matter to modern sediments is expected to be exclusively marine, in particular considering the water depth at the sampling sites (~1200 m). This expectation was confirmed by the control core $\delta^{13}C_{TOC}$, showing classical values for marine organic matter (~−2/−24‰, Gordon and Goñi, 2003). Similar $\delta^{13}C_{TOC}$ values were also measured at cores 8, 17, 19, and 21 (**Figure 2B**), even if these cores were collected at seep site and in the presence of microbial mats. Instead, the $\delta^{13}C_{TOC}$ values measured from cores 7, 9, 15, 16, 18, and 25 were very negative (ca −26 to −30‰), even compared to environments influenced by terrestrial-organic matter inputs ($\delta^{13}C_{TOC}$ = −25‰, Gordon and Goñi, 2003). We observed a negative relationship between TOC and $\delta^{13}C_{TOC}$, with more depleted carbon isotope values where the TOC is higher. A high content of microbes might be responsible for the increase of organic carbon content and a more depleted $\delta^{13}C_{TOC}$ signature due to the $\delta^{13}C$ signature of microbes fixing CO_2. However, cores 8, 17, and 19 do not fit with this relationship, suggesting a different microbial content, probably due to a different methane transport between these two groups of cores. This different microbial composition was characterized in these three cores by a higher organic carbon content with a more classical isotopic signal typical of marine environments (e.g., ~−25‰). Consequently, our $\delta^{13}C_{TOC}$ results revealed two groups of cores within the Lunde and Lomvi pockmarks: "group 1," corresponding to cores showing classical marine $\delta^{13}C_{TOC}$ values (cores 8, 17, 19, 20, and 21); and "group 2," corresponding to cores with depleted $\delta^{13}C_{TOC}$ (cores 7, 9, 15, 16, 18, and 25). This depleted $\delta^{13}C_{TOC}$ values measured in the group 2 were in the range observed in marine sediments characterized on organic carbon synthetized through the fixation of inorganic carbon by microorganisms (Ruby et al., 1987; Freeman et al., 1990; Fang et al., 1993), similar to the mat-forming microbes described in this study (Sievert et al., 2007; Grunke et al., 2012).

The push cores collected in the Lunde and Lomvi pockmarks were also analyzed in a previous study focusing on foraminiferal geochemistry ($\delta^{13}C$ and $\delta^{18}O$; Mg content; Dessandier et al., under review). In this study, the authors showed pore water profiles revealing a sharp decrease of dissolved sulfate with increasing sediment depth. In addition, dissolved inorganic carbon (DIC) depleted $\delta^{13}C$ values highlighted a high methane concentration in all the cores analyzed (except in core 20) (**Table 1**). Pore water data showed the presence of the sulfate-methane transition zone (SMTZ) within the first 10 cm in all cores, indicating methane advection at the sampling sites (**Table 1**). However, we cannot exclude that the pockmarks are also characterized by longer methane diffusive phases, since the area is covered by extensive microbial mats, which are usually absent in advective systems (Boetius and Suess, 2004). Sulfate and $\delta^{13}C_{DIC}$ profiles suggested current methane advection in cores 8 and 21 (Yao et al., 2019; Dessandier et al., under review) or lateral mechanic transport of methane due
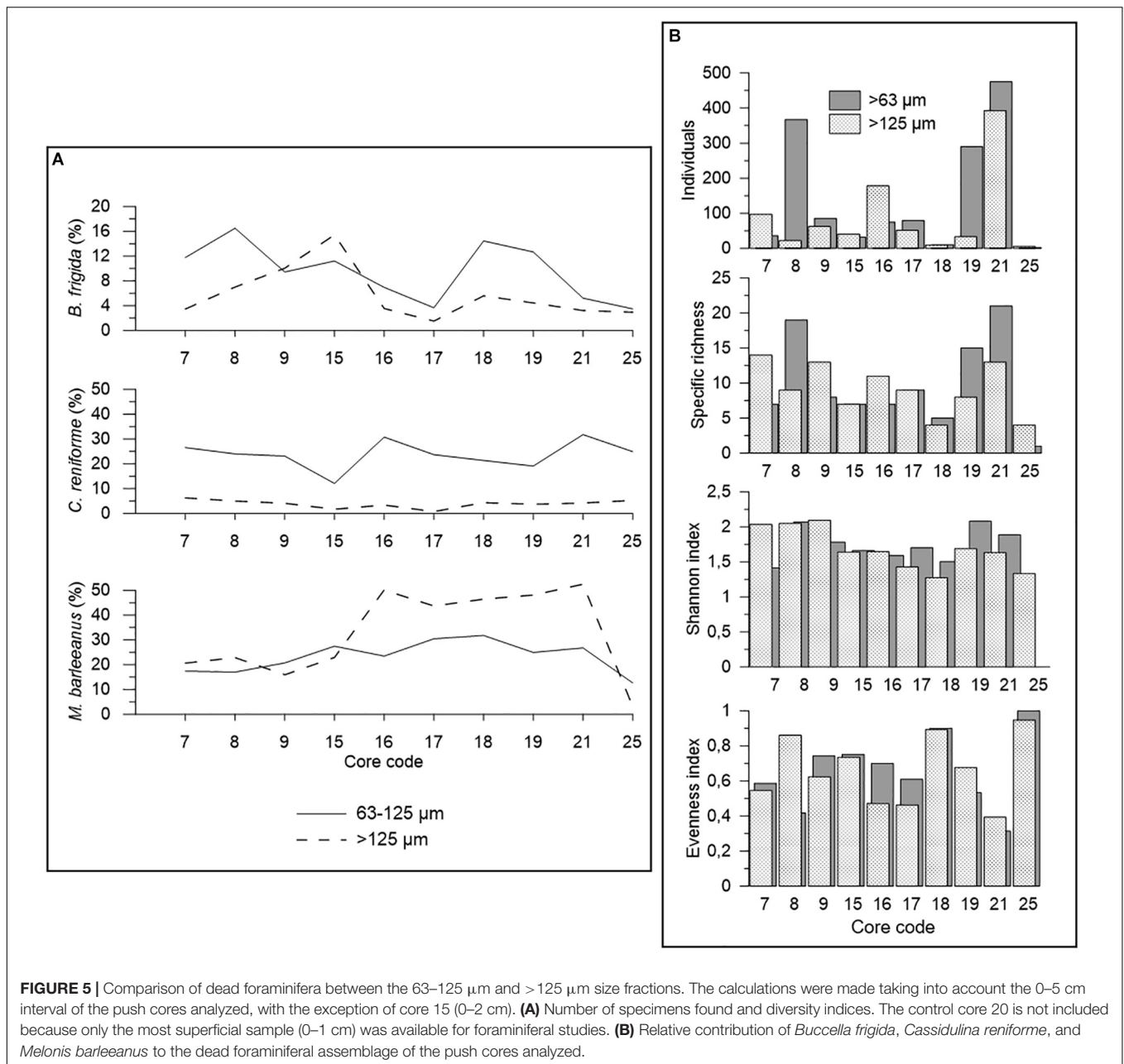
TABLE 2 | Dry sediment mass (g) of all analyzed samples.

Push core code	Sediment depth (cm)				
	0–1	1–2	2–3	3–4	4–5
7	0.38	1.02	1.89	2.47	
8	0.10	0.14	0.58	1.45	0.88
9	1.64	2.34	2.37	0.81	
15	4.38	4.85			
16	5.34	5.36	5.72	2.12	2.67
17	0.40	0.89	0.35	0.17	
18	0.69	1.86	1.66	2.04	0.71
19	0.69	1.50	1.59	1.17	0.87
20	0.50				
21	0.91	0.59	1.07	0.84	
25	1.67	1.13	1.10	0.65	0.49

Measurements were conducted on the fraction > 63 μm.

to strong advective seawater flow (Hong et al., 2016), while diffusion was likely dominant in the other cores. The two different methane transport mechanisms (advection vs. diffusion) have a different physical impact on the sediment geochemistry. Methane advection implies that methane is partially transported as free gas into bubbles, as the active phase of seepage (Hong et al., 2018) but also transport of dissolved methane in pore water (Whiticar, 1999). When methane is rapidly ascending, aqueous flow is restricted, and solutes in pore waters are only inefficiently transported by diffusion (Hong et al., 2018). Methane transport via bubbles increases the exchange between bottom seawater and pore fluid and promotes the precipitation of shallow gas hydrate (Hong et al., 2017). These unstable conditions result in less intense microbial activity, as suggested by $\delta^{13}C_{TOC}$ in cores from group 1. On the contrary, a stable methane diffusion corresponds to slow and stable molecular transport through sediments, which leads to a smoother chemical gradient. Because of this, CO_2 and sulfide fixing microbes can thrive in environments characterized by methane diffusion compared to methane advection, as demonstrated by the distribution microbial mats at Hydrate Ridge (Boetius and Suess, 2004). Here, extensive areas of microbial mats were not located at the ridge crest, where discrete gas discharge were observed (i.e., methane advection). Instead, mats were observed around the crest, where stable diffusive methane provided sulfide for microbes.

In this study, all push cores analyzed were collected in sediment covered by white and gray colored microbial mats, with the exception of the control core 20 (**Figure 2A**), where no ascending bubbles were observed. The presence of microbial mats is well known to indicate aerobic and anaerobic methane oxidation in sediments (Treude et al., 2003; Niemann et al., 2006; Hu et al., 2012). Below these mats, a major portion of methane diffusing through the sediment is anaerobically oxidized to CO_2 by archaea, using the reverse methanogenesis pathway coupled with the reduction of sulfate diffusing from seawater (Boetius et al., 2000). Consequently, sediments above the SMTZ are enriched in hydrogen sulfide and depleted in methane. In these conditions, mat formed by sulfide-oxidizing bacteria

FIGURE 5 | Comparison of dead foraminifera between the 63–125 μm and >125 μm size fractions. The calculations were made taking into account the 0–5 cm interval of the push cores analyzed, with the exception of core 15 (0–2 cm). **(A)** Number of specimens found and diversity indices. The control core 20 is not included because only the most superficial sample (0–1 cm) was available for foraminiferal studies. **(B)** Relative contribution of *Buccella frigida*, *Cassidulina reniforme*, and *Melonis barleeanus* to the dead foraminiferal assemblage of the push cores analyzed.
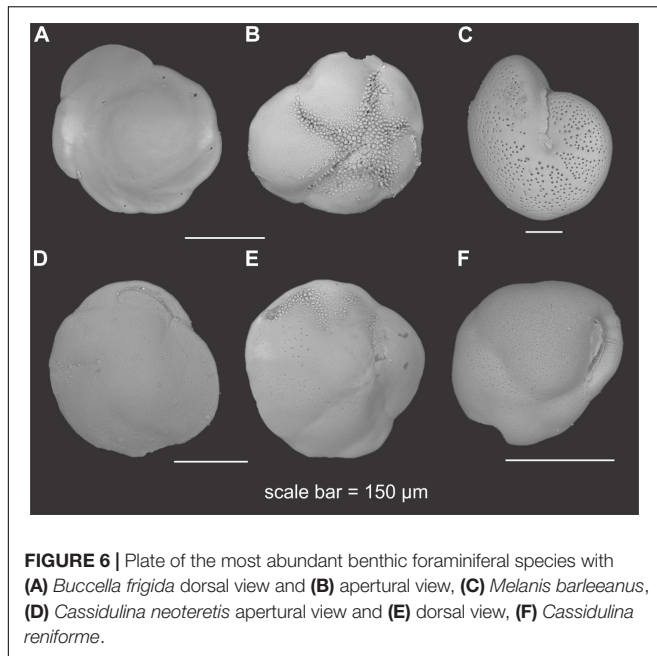
can develop (de Beer et al., 2006; Grunke et al., 2011). For example, Sahling et al. (2002) showed that the distribution of benthic communities at Hydrate Ridge is related mainly to the sulfide fluxes from surface sediments, which are regulated by the supply of methane from deeper sediment column and sulfate from seawater. White and gray mats were observed at many locations characterized by methane escaping the seafloor, like the Namibian shelf (Schulz, 2006), the Mediterranean Sea (Girnth et al., 2011), Hydrate Ridge (Torres et al., 2002), Monterey Bay (Kurt and Barry, 1998) and Håkon Mosby mud volcano (Grunke et al., 2012). Gray mats were observed in transition zones from unsteady environments characterized by very active to less active seeps, with important chemical gradient fluctuations

(de Beer et al., 2006; Felden et al., 2010). These mats were composed by *Arcobacter* spp. and *Thiomargarita* spp., which are known to be first colonizer in microbial mats at dynamic sulfidic habitats (Schulz, 2006; Sievert et al., 2007; Girnth et al., 2011; Kalenitchenko et al., 2016). On the contrary, white mats are dominated by filament forming *Beggiatoa* spp. (Grunke et al., 2012), which prefers stable sulfide and oxygen gradients (Nelson et al., 1986; Preisler et al., 2007) and low sulfide concentrations (<1 μM; Preisler et al., 2007).

Consequently, cores from group 1 correspond to the absence of methane (core 20) or to unstable methane transport due to occasionally abrupt intense fluxes (cores 8 in Lomvi, cores 17, 19, and 21 in Lunde) that lead to black/gray microbial mat cover,

FIGURE 6 | Plate of the most abundant benthic foraminiferal species with
(A) *Buccella frigida* dorsal view and **(B)** apertural view, **(C)** *Melanis barleeanus*,
(D) *Cassidulina neoteretis* apertural view and **(E)** dorsal view, **(F)** *Cassidulina reniforme*.

dominated most likely by *Arcobacter* spp. and *Thiomargarita* spp. and unstable sulfide, and likely oxygen, conditions. On the contrary, cores from group 2 collected in Lunde and Lomvi (cores 7, 9, 15, 16, 18, and 25) are characterized by more steady-methane diffusion. There, the seafloor was to be covered by white microbial mats, corresponding probably to *Beggiatoa* spp. thriving on stable sulfide and oxygen conditions. Because of this, cores from group 2 are characterized by depleted $\delta^{13}C_{TOC}$.

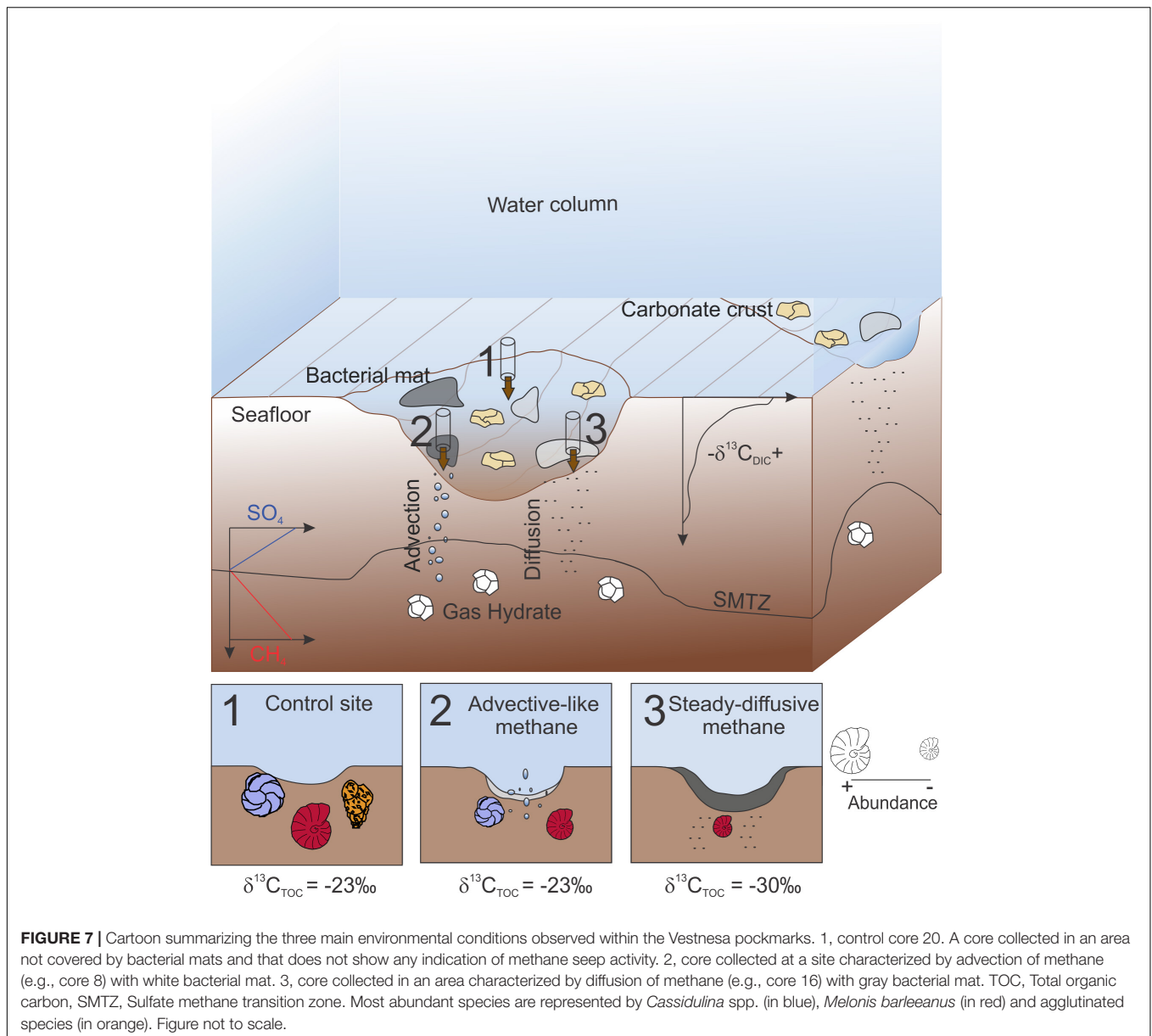## Foraminiferal Response to Gas Charged Sediments

The unique data set from Vestnesa Ridge provide the opportunity to understand the impact that the geochemical conditions at active seepage sites have on the foraminiferal distribution. Hitherto, studies conducted on benthic foraminifera from methane seep sites showed contrasting evidences on faunal density and diversity. Some authors indicated that foraminifera are more abundant and/or less diverse in seep sites, whereas other asserted the contrary (Akimoto et al., 1994; Sen Gupta and Aharon, 1994; Sen Gupta et al., 1997, 2002, 2007; Rathburn et al., 2000, 2003; Bernhard et al., 2001; Hill et al., 2003; Torres et al., 2003; Panieri, 2006; Martin et al., 2007; Panieri and Sen Gupta, 2008). These contrasting observations depend on the location of the samples available for the study (i.e., proximity to the active vent) as well as on the food availability at the sampling sites. For example, in cold seep areas from Mediterranean Sea or California Margin, benthic foraminiferal taxa from genera *Uvigerina*, *Bolivina*, *Globublimina*, *Chilostomella*, or *Nonionella* are attracted to the high availability of food (e.g., Rathburn et al., 2000; Panieri, 2006). On the contrary, oligotrophic species, such as agglutinants, are less abundant and diverse in cold seeps from Blake Ridge or offshore New Zealand (Panieri and Sen Gupta, 2008; Martin et al., 2010). Regardless some differences, all the

studies investigating the benthic foraminiferal assemblages at seep sites concluded that there are no endemic species in methane charged sediments, which was confirmed in our observations. In fact, in both dead and living communities, individuals found in Lunde and Lomvi pockmarks represent classical species often observed in the Arctic Ocean (e.g., *Cassidulina* spp., *Cibicidoides* spp., *M. barleeanus*; Hald and Korsun, 1997; Wollenburg and Kuhnt, 2000).

Microhabitat controls faunal distribution (density and diversity) mainly through its physical and chemical properties like grain size, oxygen depletion, and source, quantity, and quality of the organic matter stocked in the sediment (e.g., Jorissen et al., 1995; Schönfeld, 2002; Dessandier et al., 2016). The impact of organic content on benthic foraminiferal density and diversity is unclear at the locations of this study. Indeed, the richest cores in TOC ("group 1" cores 8 and 19 from Lomvi and Lunde, respectively) show higher numbers of living individuals compared to the other methane-related cores, but the highest foraminiferal density and diversity is observed in the control core 20, characterized by the lowest TOC values of this study (**Figures 3**, **4**). Wollenburg and Kuhnt (2000) estimated that benthic foraminiferal distribution is correlated with carbon flux for fluxes < 7gC m^{-2} y^{-1} or ~1.5% of TOC. The control core TOC measured in the present study is of 1.5%, arguing that the organic carbon stock at Vestnesa Ridge is not a limiting factor. In this core, the foraminiferal diversity is dominated by agglutinated species. Instead, all the push cores collected in methane charged sediments are characterized by the occurrence of eutrophic species because of the higher organic content in these cores.

At cold seep sites, it was proposed that sulfide-rich sediments can represent a toxic environment for benthic foraminifera (Akimoto et al., 1994; Bernhard et al., 2001). However, the presence of living foraminifera was reported at cold seeps with sulfide concentrations exceeding 16 mM (Rathburn et al., 2003), indicating a high tolerance of certain species (e.g., *U. peregrina*, *Globobulimina* spp.) to sulfide. The pore water sulfate profiles from our push cores (Dessandier et al., under review) showed a sharp decrease of sulfate with sediment depth, which resulted in high sulfide concentrations close to the sediment surface (0–5 cm). Consequently, surface sediments at Lunde and Lomvi can be potentially toxic for benthic foraminifera. Although *U. peregrina* and *Globobulimina* spp. were not observed in our cores, we found high abundance of the intermediate infaunal species like *M. barleeanus*, which might also be sulfidic-tolerant and has been found living down to 4 cm within the SMTZ (core 8).

Another possible hostile condition at seep environments is represented by the high pCO$_2$ due to methane oxidation close to the seafloor, which could restrain foraminiferal calcification or dissolve their calcareous tests (Herguera et al., 2014). Calcite dissolution due to high pCO$_2$ might result in a larger proportion of agglutinated species in sediments (Herguera et al., 2014). The visual observation of abundant planktonic foraminifera, especially the species *Neogloboquadrina pachyderma* in all investigated samples suggested a low calcite dissolution at the sampling sites. Among all the cores analyzed, the higher foraminiferal density and diversity detected in cores 8 and 20

FIGURE 7 | Cartoon summarizing the three main environmental conditions observed within the Vestnesa pockmarks. 1, control core 20. A core collected in an area not covered by bacterial mats and that does not show any indication of methane seep activity. 2, core collected at a site characterized by advection of methane (e.g., core 8) with white bacterial mat. 3, core collected in an area characterized by diffusion of methane (e.g., core 16) with gray bacterial mat. TOC, Total organic carbon, SMTZ, Sulfate methane transition zone. Most abundant species are represented by *Cassidulina* spp. (in blue), *Melonis barleeanus* (in red) and agglutinated species (in orange). Figure not to scale.

might be partially due to the presence of agglutinated species. Core 20 was not affected by methane release and oxidation, so in this core a high abundance of agglutinated foraminifera was not related to dissolution of calcareous ones, but most likely to the absence of methane. Calcareous species were dominant in all the other cores, suggesting that methane oxidation was not responsible for the dissolution of calcareous species at the locations of this study.

In the Arctic Ocean, agglutinated species are often observed to be the dominant component of the foraminiferal assemblages, showing a preference for oligotrophic conditions and degraded organic matter (Wollenburg and Mackensen, 1998; Jernas et al., 2017). Agglutinated foraminifera represent also a critical proportion of species in the deep-sea food web (Gooday et al., 2005) and some of them (e.g., *Saccammina* spp., *Rhabdammina*

spp.) are known to recolonize sediments after oxygen depletion and/or carbonate dissolution (Wollenburg et al., 2001), but are classically poorly preserved as fossils (Goineau et al., 2015; Dessandier et al., 2018). Agglutinated species were most abundant in the control core, with a high percentage of living *Reophax* spp. (*Reophax scorpiurus*, *Reophax bilocularis*, *Reophax guttifera*) and *Recurvoides turbinatum* in a few cores (group 1: cores 8, 19, and control core 20). Species from the genus *Reophax* are fragile and it is unlikely that they can be preserved in the fossil record of Vestnesa Ridge. Surprisingly, *R. turbinatum* specimens were well preserved in the first 5 cm of sediment depth, even though it was observed that this species could rarely be preserved as fossil (Belanger and Streeter, 1980). Despite their fragility, the absence of agglutinated species in superficial sediment of most of the cores analyzed, especially group 2,

could be due to: (1) the larger relative contribution of calcareous species to the foraminiferal assemblages in the pockmarks of Vestnesa Ridge; (2) higher competition limiting the distribution of agglutinated species; and/or (3) the geochemical conditions at methane seeps limit the survival of agglutinated foraminifera, as already observed at other methane seeps at Hydrate Ridge and Blake Ridge (Heinz et al., 2005; Panieri and Sen Gupta, 2008). The presence of agglutinants, which are oligotrophic species, explained the higher density and diversity at the control site, where the TOC was lower than at methane charged sediment. The organic matter provided by the dynamic biology in methane charged sediments allowed the eutrophic-tolerant species to be more successful, with assemblages dominated by *M. barleeanus* and/or *Casssidulina* spp. The dominance of these species and very low abundances of agglutinants hence represent the main characteristics of methane-rich sediment in the area.

Low faunal densities were observed in the living community of cores classified as group 2, whereas a significant number of living individuals was found in cores of group 1. In group 1 cores, species like *C. neoteretis*, *B. frigida,* and *C. reniforme* were the most abundant. These species are usually dominant at Vestnesa Ridge (Sztybor and Rasmussen, 2017a,b; Consolaro et al., 2018) and our results confirm their tolerance to the environmental conditions of methane charged sediments. *C. neoteretis* was the most abundant species in samples collected at Vestnesa Ridge (e.g., Consolaro et al., 2015, 2018; Sztybor and Rasmussen, 2017a,b). This species is known to feed on bacteria and is usually correlated with high carbon fluxes (Wollenburg et al., 2004). Interestingly, *B. frigida* was described as controlled by seasonal sea ice due to its feeding preferences (i.e., fresh algae; Seidenkrantz, 2013). However, the occurrence of *B. frigida* in samples from Vestnesa pockmarks suggested that this species can also feed on microbial food source. The additional carbon supply represented by microbial mats at seeps might trigger the abundance of *B. frigida*, which responds to elevated fluxes of organic matter in the Arctic Ocean (Polyak et al., 2002). *C. reniforme* is commonly associated with cold periods and/or proximity to glaciers (Hald and Korsun, 1997) preferring cool and saline waters (Jernas et al., 2017), which correspond to the characteristics of the deep-water mass bathing Vestnesa Ridge (T = 0–2°C, S = 35; Hirche, 1991). This species was the only one inhabiting the microbial mats in the Håkon Mosby Mud Volcano and was described as a methane and dysoxic-tolerant species (Wollenburg and Mackensen, 2009).

Wollenburg and Mackensen (2009) argued for a control of oxygen depletion on the foraminiferal distribution at cold seeps, with absence of most of species due to anoxic conditions within bacterial mats. A strong oxygen depletion within bacterial mats could explain the low faunal densities found in cores from group 2, where the surface may be depleted in oxygen due to microbial activity. Unfortunately, the lack of oxygen concentration data from these cores prevents us from drawing a firm conclusion regarding this possibility. However, we note that at other cold seep areas, like Blake Ridge (Panieri and Sen Gupta, 2008), Monterey Bay (Bernhard et al., 2001), and Hydrate Ridge (Torres et al., 2003; Heinz et al., 2005), oxygen depleted and high sulfide (e.g., microbial mats) does not prevent the presence of eutrophic

and anoxic-tolerant species (e.g., *U. peregrina*, *Bolivina* spp.) within the first centimeters of sediment.

All the most abundant species observed in the present study are known to live in organic-rich sediments in the Arctic Ocean (Mackensen and Hald, 1988; Wollenburg et al., 2001, 2004), suggesting a control of high carbon stock, provided by microbes feeding on methane or sulfide. *M. barleeanus* is the most abundant species in cores from group 2. Microbial mats probably represent a food source for this species, which is indicative of high content of degraded organic matter (Wollenburg et al., 2004; Dijkstra et al., 2015), as observed also at another methane seepage off Niger (Fontanier et al., 2014). Recently, a putative symbiosis between microbes and *M. barleeanus* was reported for samples from Vestnesa Ridge (Bernhard and Panieri, 2018), suggesting that this species benefits from its association with methanotrophic bacteria. This could suggest that methane advection could enhance the development of particular methanotrophic bacterial species that contribute for symbiotic association with *M. barleeanus*. More work needs to be done to determine what kind of symbiotic relationship exist between methanotrophic bacteria and benthic foraminiferal species (Bernhard and Panieri, 2018), but the conditions related to methane transport most likely impact the microbial community and indirectly benthic foraminiferal distribution through feeding strategy and/or symbiosis with bacteria.

All cores from group 2 show low densities of dead fauna in the first centimeter of sediment (**Figure 4**). This pattern was already observed in one core from the northern California margin, where the benthic foraminiferal density was surprisingly low above 1 cm (Rathburn et al., 2000). However, this vertical distribution is unusual at both non-seep and cold seep environments (e.g., Torres et al., 2003; Heinz et al., 2005; Dessandier et al., 2018). In general, benthic foraminifera can present very patchy distributions depending on the substrate characteristics (e.g., grain size, presence of rocks), which are more diversified at seep sites. This could explain the unusual vertical distribution observed, with accumulation of individuals in sediment pockets, even if we note that physical characteristics cannot explain the systematic low abundance of dead foraminifera in surface samples from group 2 (cores 7, 9, 15, 16, 18, and 25). Rathburn et al. (2003) proposed that fauna might be attracted by the seep chemistry or biota corresponding to subsurface conditions, characterized by more widespread bacterial food source. To our knowledge, the preference of foraminiferal species for *Arcobacter* spp., *Thiomargarita* spp. or *Beggiatoa* spp., which are typical of seepage sites, has not been investigated before.

The benthic foraminiferal preference for different microbial species and/or the competition with microbes for organic matter mineralization can affect the foraminiferal distribution (i.e., density and diversity). In this context, it is possible that the microbial activity at surface sediment affects the benthic foraminiferal distribution, mineralizing all the labile organic matter and/or creating a toxic environment (i.e., high pCO_2 or high sulfide concentration) for benthic foraminifera, as suggested by Herguera et al. (2014). On the other hand, if benthic foraminifera are sulfide tolerant, as suggested by Rathburn et al. (2003), then the most plausible explanation for our vertical

profiles and faunal distribution would be the different chemical conditions (i.e., stability of sulfide and oxygen fluxes) driven by methane transport.

In summary, in this study we present the environmental conditions observed at two Vestnesa pockmarks and their impact on the foraminiferal distribution (**Figure 7**). Within the same pockmark, control-like conditions (**Figure 7-1**) are characterized by sediment with classical Arctic marine organic matter content and isotopic signature (i.e., TOC ~1.5%, $\delta^{13}C_{TOC}$ ~24‰) and high faunal density and diversity, particularly due to the abundance of agglutinated species. In sediments characterized by methane advection (**Figure 7-2**), which corresponds to unstable sulfide and oxygen conditions (cores from group 1), eutrophic-tolerant species and opportunistic species (*Cassidulina* spp.) use the microbial food source to thrive. Even so, the foraminiferal density and diversity is lower than at the control site because of the low abundance of agglutinated species. At steady-diffusive methane systems (cores from group 2) (**Figure 7-3**), white mats cover the sediment where sufficient sulfide is provided for intense microbial activity resulting in depleted $\delta^{13}C_{TOC}$ and high TOC. These conditions restrain the foraminiferal distribution, drastically decreasing the diversity. In these sediments, *M. barleeanus* is the most abundant species. Our results highlight the potential use of benthic foraminiferal assemblages to better understand the methane dynamics. In particular, abundance of agglutinated species and variability in the benthic foraminiferal density and diversity can be used to reconstruct the dynamic of methane release.

Impact of Size Fraction on Foraminiferal Assemblages

In the Arctic, the benthic foraminiferal assemblages were studied in many locations, like the Yermak Plateau (e.g., Wollenburg et al., 2001, 2004), Baffin Bay (e.g., Seidenkrantz, 2013), and the Barents Sea (e.g., Rasmussen et al., 2007). The goal of these investigations was to reconstruct changes in paleoceanographic conditions, such as paleoproductivity, sea-ice cover, and ocean circulation. However, the methodology used was different depending on the geographic area or the focus of the study. In particular, we note that the size fractions used varied from >63, >100, >125, >150, to >250 μm. Benthic foraminiferal assemblages were investigated at Vestnesa Ridge, as well, by examining the foraminifera in the >100 μm size fraction only (Sztybor and Rasmussen, 2017a,b; Consolaro et al., 2018).

In this study, the identification of living and dead individuals from different size fractions reveals a potential size bias when investigating benthic foraminiferal assemblages in Arctic sediments. In fact, certain species indicative of environmental changes (e.g., *C. reniforme*) are often very small (~70 μm). Also, during permanent sea-ice cover, benthic foraminifera show an average size of 70 μm (Wollenburg and Mackensen, 1998). The comparison of the size fractions >63 and >125 μm of surface samples (0–1 cm) from push cores collected at Vestnesa Ridge (**Figure 5**) shows that the abundance and diversity of at least three of the major species commonly used for paleoceanographic reconstructions (*B. frigida*, *C. reniforme*, *M. barleeaus*) depends

on the size fraction observed. For instance, cold-polar water and glacio-marine conditions characterize the habitat of *C. reniforme* (Sejrup and Guibault, 1980; Mudie et al., 1984; Hald and Vorren, 1987; Polyak and Solhelm, 1994; Seidenkrantz, 1995). In some studies, the abundance of *C. reniforme* was used to reconstruct the occurrence of cold bottom water masses at Vestnesa Ridge; however, only the size fraction >100 μm was analyzed (Sztybor and Rasmussen, 2017a,b; Consolaro et al., 2018). Our data demonstrate that this species is always significantly more abundant in the 63–125 μm size fraction, suggesting a potentially strong bias in the interpretation of geological records when the finer fraction is not considered. In this context, focusing on the larger size fraction would lead to an underestimation of episodes of cold bottom water, changes in ocean circulation, and stadial/interstadial interpretations. The abundance of other palaeoceanographically relevant species can be influenced by the size fraction selected for analysis. For example, the relative contribution of *M. barleeanus* can be overestimated when using the coarse fraction (>100/125 μm) only.

Based on our results, we conclude that the use of the >100 μm size fraction, which is commonly used in Arctic paleoceanographic studies, might affect the interpretation of the fossil record as it might lack part of the environmental signal. In addition, the use of the fraction >100 μm makes the comparison of between studies conducted in Arctic environments and studies conducted in other regions challenging because traditionally benthic foraminiferal assemblages data are reported as the fraction >63 and >125 μm. We suggest that ecological studies based on benthic foraminifera in the Arctic should always consider the >63 μm size fraction.

CONCLUSION

This study provided crucial information regarding the interpretation of benthic foraminiferal assemblages in Arctic methane seeps. Our data confirmed that common arctic species (e.g., *C. neoteretis*, *C. reniforme*, *M. barleeanus*) are able to live in environments currently releasing methane, like the Lunde and Lomvi pockmarks at Vestnesa Ridge. Faunal assemblages show higher density and diversity in the control core, which is unaffected by methane release and is lacking microbial mats. Here, the benthic foraminiferal assemblage is mainly composed by agglutinated species. Thus, marine environments characterized by dynamic methane emissions, the abundance of agglutinated species in the fossil record can indicate the end (or the absence) of methane emission at the seafloor.

Benthic foraminiferal calcareous species, such as *M. barleeanus* and *C. neoteretis*, show high abundance in methane charged sediments, probably as a consequence of food provided by methane-related microbes. This highlights that benthic foraminiferal abundance and diversity are very likely affected by methane seepages. Low faunal abundance was observed and correlated with environments characterized by methane diffusion. In methane-diffusive areas, the environment might be poisonous to foraminifera because of the constant and high sulfide concentration, or possibly the strong

microbial activity restrains the benthic foraminiferal activity in surface microhabitats.

In the light of our results, benthic foraminiferal assemblages could provide information on methane release events in the Arctic Ocean looking at:

- relative contribution of agglutinated vs. opportunistic species: agglutinated species are dominant in the Arctic except where/when there is a methane charged sediment or organic matter input related to the methane supply and related microbial mats;
- diversity variations: the faunal diversity is reduced in methane charged sediments;
- variable faunal density: usually stable on short time scales, changes in fossil densities can be related to toxic environments linked with strong microbial activities and degraded organic matter during diffusion of methane.

Finally, a comparison between the 63–125 μm and >125 μm size fractions highlighted the importance of analyzing the fine fraction for benthic foraminiferal ecology in the Arctic Ocean. All these observations are particularly important in order to reconstruct methane release in the past using fossil assemblages that would provide evidences to compare/combined with stable isotopes measured on foraminiferal tests. Considering the importance of understanding the dynamic of methane release and its connection with climates, this study confirms the very useful application of benthic foraminifera.

Future investigations on the diet of benthic foraminifera in cold seeps should be conducted to better understand the influence of food availability on foraminiferal distribution at cold seeps. In addition, studies investigating the potential influence of the microbial mat on the benthic foraminiferal abundance and diversity would be fundamental to determine if there are species-specific preferences for methane-related microbes. This knowledge could potentially allow the setup of culturing experiments aimed to better understand the benthic foraminiferal response to seep activity. For instance, a recent study highlighted the potential symbiotic relationship between benthic foraminifera and methanotrophic bacteria (Bernhard and Panieri, 2018), even if what kind of symbiosis remains to be determined. Overall, this knowledge would improve our ability to use this group of organisms as bio-indicators of methane transport and seep activity.

DATA AVAILABILITY STATEMENT

The datasets generated for this study can be found in the **Supplementary Material**.

AUTHOR CONTRIBUTIONS

P-AD and GP designed the study. GP collected the samples. P-AD carried out the laboratory work and analyzed the data. P-AD, CB, and DK wrote the manuscript. All authors commented on and contributed to the various versions of the manuscript.

SUPPLEMENTARY MATERIAL

The Supplementary Material for this article can be found online at: https://www.frontiersin.org/articles/10.3389/fmars.2019.00765/full#supplementary-material

REFERENCES

Aagaard, K., Foldvik, A., and Hillman, S. R. (1987). The west Spitsbergen current: disposition and water mass transformation. *J. Geophys. Res.* 92, 3778–3784.

Akimoto, K., Tanaka, T., Hattori, M., and Hotta, H. (1994). "Recent benthic foraminiferal assemblages from the cold seep communities — a contribution to the methane gas indicator," in *Pacific Neogene Events in Time and Space*, ed. R. Tsuchi, (Tokyo: University of Tokyo Press), 11–25.

Belanger, P. E., and Streeter, S. S. (1980). Distribution and ecology of benthic foraminifera in the Norwegian-Greenland Sea. *Mar. Micropaleontol.* 5, 401–428. doi: 10.1016/0377-8398(80)90020-1

Bernhard, J. M., and Panieri, G. (2018). Keystone Arctic paleoceanographic proxy association with putative methanotrophic bacteria. *Sci. Rep.* 8:10610. doi: 10.1038/s41598-018-28871-3

Bernhard, J. M., Buck, K. R., and Barry, J. P. (2001). Monterey Bay cold-seep biota: assemblages, abundance, and ultrastructure of living foraminifera. *Deep Sea Res. Part I* 48, 2233–2249. doi: 10.1016/s0967-0637(01)00017-6

Bernhard, J. M., Martin, J. B., and Rathburn, A. (2010). Combined carbonate carbon isotopic and cellular ultrastructural studies of individual benthic foraminifera: 2. Toward an understanding of apparent disequilibrium in hydrocarbon seeps. *Paleoceanography* 25, A4206. doi: 10.1029/2010PA001930

Boetius, A., and Suess, E. (2004). Hydrate Ridge: a natural laboratory for the study of microbial life fueled by methane from near-surface gas hydrates. *Chem. Geol.* 205, 291–310. doi: 10.1016/j.chemgeo.2003.12.034

Boetius, A., Ravenschlag, K., Schubert, C. J., Rickert, D., Widdel, F., Gieseke, A., et al. (2000). A marine microbial consortium apparently mediating anaerobic oxidation of methane. *Nature* 407, 623–626. doi: 10.1038/3503 6572

Bünz, S., Polyanov, S., Vadakkepuliyambatta, S., Consolaro, C., and Mienert, J. (2012). Active gas venting through hydrate-bearing sediments on the Vestnesa Ridge, offshore W Svalbard. *Mar. Geol.* 33, 189–197. doi: 10.1016/j.margeo.2012.09.012

Consolaro, C., Rasmussen, T. L., and Panieri, G. (2018). Palaeoceanographic and environmental changes in the eastern Fram Strait during the last 14,000

years based on benthic and planktonic foraminifera. *Mar. Micropaleontol.* 139, 84–101. doi: 10.1016/j.marmicro.2017.11.001

Consolaro, C., Rasmussen, T. L., Panieri, G., Mienert, J., Bünz, S., and Sztybor, K. (2015). Carbon isotope (δ^{13}C) excursions suggest times of major methane release during the last 14 kyr in Fram Strait, the deepwater gateway to the Arctic. *Clim Past* 11, 669–685. doi: 10.5194/cp-11-669-2015

Corell, R. W., Hassol, S. J., and Melillo, J. (2008). *Emerging Challenges – Methane from the Arctic: Global warming wildcard, UNEP Year Book 2008: An Overview of Our Changing Environment.* Stevenage: United Nations Environment Programme.

Corliss, B. H. (1991). Morphology and microhabitat preference of benthic foraminifera from the northwest Atlantic Ocean. *Mar. Micropaleontol.* 17, 195–236. doi: 10.1016/0377-8398(91)90014-W

de Beer, D., Sauter, E., Niemann, H., Kaul, N., Foucher, J.-P., Witte, U., et al. (2006). In situ fluxes and zonation of microbial activity in surface sediments of the Håkon Mosby Mud Volcano. *Limnology and Oceanography* 51, 1315–1331. doi: 10.4319/lo.2006.51.3.1315

Decho, A. W., and Gutierrez, T. (2017). Microbial extracellular polymeric substances (EPSs) in ocean systems. *Front. Microbiol.* 8:922. doi: 10.3389/fmicb.2017.00922

Dessandier, P.-A., Bonnin, J., Kim, J.-H., and Racine, C. (2018). Comparison of living and dead benthic foraminifera on the Portuguese Margin: understanding the taphonomical processes. *Mar. Micropaleontol.* 140, 1–16. doi: 10.1016/j.marmicro.2018.01.001

Dessandier, P.-A., Bonnin, J., Kim, J.-H., Bichon, S., Deflandre, B., Grémare, A., et al. (2016). Impact of organic matter source and quality on living benthic foraminiferal distribution on a river-dominated continental margin: a study of the Portuguese margin. *J. Geophys. Res. Biogeosci.* 121, 1689–1714. doi: 10.1002/2015jg003231

Dijkstra, N., Junttila, J., Husum, K., Carroll, J., and Hald, M. (2015). Natural variability of benthic foraminiferal assemblages and metal concentrations during the last 150 years in the Ingøydjupet trough. SW Barents Sea. *Mar. Micropaleontol.* 121, 16–31. doi: 10.1016/j.marmicro.2015.09.005

Eiken, O., and Hinz, K. (1993). Contourites in the Fram Strait. *Sediment. Geol.* 82, 15–32. doi: 10.1016/0037-0738(93)90110-q

Elverhøi, A., Andersen, E. S., Dokken, T., Hebbeln, D., Spielhagen, R., Svendsen, J. I., et al. (1995). The growth and decay of the Late Weichselian ice sheet in western Svalbard and adjacent areas based on provenance studies of marine sediments. *Quat. Res.* 44, 303–316. doi: 10.1006/qres.1995.1076

Fang, J., Abrajano, T. A., Comet, P. A., Brooks, J. M., Sassen, R., and MacDonald, I. R. (1993). Gulf of Mexico hydrocarbon seep communities: XI. Carbon isotopic fractionation during fatty acid biosynthesis of seep organisms and its implication for chemosynthetic processes. *Chem. Geol.* 109, 271–279. doi: 10.1016/0009-2541(93)90074-s

Felden, J., Wenzhöfer, F., Feseker, T., and Boetius, A. (2010). Transport and consumption of oxygen and methane in different habitats of the Håkon Mosby Mud Volcano (HMMV). *Limnol. Oceanogr.* 55, 2366–2380. doi: 10.4319/lo.2010.55.6.2366

Fontanier, C., Koho, K. A., Goñi-Urriza, M. S., Deflandre, B., Galaup, S., Ivanovsky, A., et al. (2014). Benthic foraminifera from the deep-water Niger delta (Gulf of Guinea): assessing present-day and past activity of hydrate pockmarks. *Deep Sea Res. I* 94, 87–106. doi: 10.1016/j.dsr.2014.08.011

Freeman, K. H., Hayes, J. M., Trendel, J.-M., and Albrecht, P. (1990). Evidence from carbon isotope measurements for diverse origins of sedimentary hydrocarbons. *Nature* 343, 254–256. doi: 10.1038/343254a0

Girnth, A. C., Grünke, S., Lichtschlag, A., Felden, J., Knittel, K., Wenzhöfer, F., et al. (2011). A novel, mat-forming thiomargarita population associated with a sulfidic fluid flow from a deep-sea mud volcano. *Environ. Microbiol.* 13, 495–505. doi: 10.1111/j.1462-2920.2010.02353.x

Goineau, A., Fontanier, C., Mojtahid, M., Fanget, A.-S., Bassetti, M.-A., Berné, S., et al. (2015). Live–dead comparison of benthic foraminiferal faunas from the Rhône prodelta (Gulf of Lions, NW Mediterranean): development of a proxy for paleoenvironmental reconstructions. *Mar. Micropaleontol.* 119, 17–33. doi: 10.1016/j.marmicro.2015.07.002

Goldstein, S. T., and Corliss, B. H. (1994). Deposit feeding in selected deep-sea and shallow-water benthic foraminifera. *Deep Sea Res. Part I* 41, 229–241. doi: 10.1016/0967-637(94)90001-9

Gooday, A. J., Bowser, S. S., Cedhagen, T., Cornelius, N., Hald, M., Korsun, S., et al. (2005). Monothalamous foraminiferans and gromiids (Protista) from western Svalbard: a preliminary survey. *Mar. Biol. Res.* 1, 290–312. doi: 10.1080/17451000510019150

Gordon, E. S., and Goñi, M. A. (2003). Sources and distribution of terrigenous organic matter delivered by the Atchafalaya River to sediments in the northern Gulf of Mexico. *Geochim. Cosmochim. Acta* 67, 2359–2375. doi: 10.1016/s0016-7037(02)01412-6

Grunke, S., Felden, J., Lichtschlag, A., Girnth, A.-C., de Beer, D., Wenhöfer, F., et al. (2011). Niche differentiation among mat-forming, sulfide-oxidizing bacteria at cold seeps of the Nile Deep Sea Fan (Eastern Mediterranean Sea). *Geobiology* 9, 330–348. doi: 10.1111/j.1472-4669.2011.00281.x

Grunke, S., Lichtschlag, A., de Beer, D., Felden, J., Salman, V., Ramette, A., et al. (2012). Mats of psychrophilic thiotrophic bacteria associated with cold seeps of the Barents Sea. *Biogeosciences* 9, 2947–2960. doi: 10.5194/bg-9-2947-2012

Hald, M., and Korsun, S. (1997). Distribution of modern benthic foraminifera from fjords of Svalbard. European Arctic. *J. Foraminiferal Res.* 27, 101–122. doi: 10.2113/gsjfr.27.2.101

Hald, M., and Vorren, T. O. (1987). Foraminiferal sratigraphy and environments of late Weichselian deposits on the continental shelf off Tromsø, northern Norway. *Mar. Micropaleontol.* 12, 129–160. doi: 10.1016/0377-8398(87)90018-1

Hammer, Ø, Harper, D. A. T., and Ryan, P. D. (2001). *PAST-Paleontological Statistics.* Available at: https://palaeo-electronica.org/2001_1/past/issue1_01.htm (accessed 25, 2009).

Heeger, T. (1990). Electronenmikroskopische Untersuchungen zur Ernlihrungsbiologie benthischerForaminiferen. *Berichte aus dem Sonderforschungsbereich* 313, 1–139.

Heinz, P., Sommer, S., Pfannkuche, O., and Hemleben, C. (2005). Living benthic foraminifera in sediments influenced by gas hydrates at the Cascadia convergent margin, NE Pacific. *Mar. Ecol. Prog. Ser.* 304, 77–89. doi: 10.3354/meps304077

Herguera, J. C., Paull, C. K., Perez, E., Ussler, W., and Peltzer, E. (2014). Limits to the sensitivity of living benthic foraminifera to pore water carbon isotope anomalies in methane vent environments. *Paleoceanography* 29, 273–289. doi: 10.1002/2013PA002457

Hill, T. M., Kennett, J. P., and Spero, H. J. (2003). Foraminifera as indicators of methane-rich environments: a study of modern methane seeps in Santa Barbara Channel. California. *Mar. Micropaleontol.* 49, 123–138. doi: 10.1016/s0377-8398(03)00032-x

Hirche, H. J. (1991). Distribution of dominant calanoid copepod species in the Greenland Sea during late fall. *Polar Biol.* 11, 351–362.

Hong, W.-L., Sauer, S., Panieri, G., Ambrose, W. G., James, R. H., Plaza-Faverola, A., et al. (2016). Removal of methane through hydrological, microbial, and geochemical processes in the shallow sediments of pockmarks along eastern Vestnesa Ridge (Svalbard). *Limnol. Oceanogr.* 61, 324–343.

Hong, W.-L., Torres, M. E., Carroll, J., Cremiere, A., Panieri, G., Yao, H., et al. (2017). Seepage from an Arctic shallow marine gas hydrate reservoir is insensitive to momentary ocean warming. *Nat. Commun.* 8:15745.

Hong, W.-L., Torres, M. E., Portnov, A., Waage, M., Haley, B., and Lepland, A. (2018). Variations in gas and water pulses at an arctic seep: fluid sources and methane transport. *Geophys. Res. Lett.* 45, 4153–4162. doi: 10.1029/2018GL077309

Howe, J. A., Shimmield, T. M., and Harland, R. (2008). Late quaternary contourites and glaciomarine sedimentation in the Fram Strait. *Sedimentology* 55, 179–200. doi: 10.1111/j.1365-3091.2007.00897.x

Hu, L., Yvon-Lewis, S. A., Kessler, J. D., and MacDonald, I. R. (2012). Methane fluxes to the atmosphere from deepwater hydrocarbon seeps in the northern Gulf of Mexico. *J. Geophys. Res.* 17:C01009. doi: 10.1029/2011JC007208

Hustoft, S., Bünz, S., Mienert, J., and Chand, S. (2009). Gas hydrate reservoir and active methane-venting province in sediments on < 20 Ma young oceanic crust in the Fram Strait, offshore NW-Svalbard. *Earth Planet. Sci. Lett.* 284, 12–24. doi: 10.1016/j.epsl.2009.03.038

Ipcc (2013). "Climate Change 2013: the physical science basis," in *Contribution of Working Group I to the Fifth Assessment Report of the Intergovernmental Panel on Climate Change*, (Cambridge: Cambridge Univ. Press).

Jernas, P., Klitgaard-Kristensen, D., Husum, K., Koç, M., Tverberg, N., Loubere, P., et al. (2017). Annual changes in Arctic fjord environment and modern benthic foraminiferal fauna: Evidence from Kongsfjorden. Svalbard. *Glob. Planet. Change* 163, 119–140. doi: 10.1016/j.gloplacha.2017.11.013

Jorissen, F. J., de Stigter, H. C., and Widmark, J. G. (1995). A conceptual model explaining benthic foraminiferal microhabitats. *Mar. Micropaleontol.* 26, 3–15. doi: 10.1016/0377-8398(95)00047-x

Judd, A., and Hovland, M. (2007). *Seabed Fluid Flow: The Impact on Geology, Biology and the Marine Environment*. Cambridge: Cambridge University Press, 475.

Kalenitchenko, D., Dupraz, M., Le Bris, N., Petetin, C., Rose, C., West, N. J., et al. (2016). Ecological succession leads to chemosynthesis in mats colonizing wood in sea water. *ISME J.* 10, 2246–2258. doi: 10.1038/ismej.2016.12

Knies, J., and Martinez, P. (2009). Organic matter sedimentation in the western Barents Sea region: terrestrial and marine contribution based on isotopic composition and organic nitrogen content. *Norwegian J. Geol.* 89, 79–79.

Knies, J., Daszinnies, M., Plaza-Faverola, A., Chand, C., Sylta, Ø., Bünz, S., et al. (2018). Modelling persistent methane seepage offshore western Svalbard since early Pleistocene. *Mar. Petrol. Geol.* 91, 800–811. doi: 10.1016/j.marpetgeo. 2018.01.020

Kurt, R. B., and Barry, J. B. (1998). Monterey Bay cold seep infauna: quantitative comparison of bacterial mat meiofauna with non-seep control sites. *Cahiers Biol. Mar.* 39, 333–335.

Linke, P., Altenbach, A. V., Graf, G., and Heeger, T. (1995). Response of deep-sea benthic foraminifera to a simulated sedimentation event. *J. Foraminiferal Res.* 25, 75–82. doi: 10.1371/journal.pone.0080510

Mackensen, A., and Hald, M. (1988). *Cassidulina teretis* Tappan and *C. laevigata* d'Orbigny; their modern and late Quaternary distribution in northern seas. *J. Foraminiferal Res.* 18, 16–24. doi: 10.2113/gsjfr.18.1.16

Martin, R. A., Nesbitt, E. A., and Campbell, K. A. (2007). Carbon stable isotopic composition of benthic foraminifera from Pliocene cold methane seeps, Cascadia accretionary margin. *Palaeogeogr. Palaeoclimatol. Palaeoecol.* 246, 260–277. doi: 10.1016/j.palaeo.2006.10.002

Martin, R. A., Nesbitt, E. A., and Campbell, K. A. (2010). The effects of anaerobic methane oxidation on benthic foraminiferal assemblages and stable isotopes on the Hikurangi Margin of eastern New Zealand. *Mar. Geol.* 272, 270–284. doi: 10.1016/j.margeo.2009.03.024

McGuire, A. D., Anderson, L. G., Christensen, T. R., Dallimore, S., Guo, L., Hayes, D. J., et al. (2009). Sensitivity of the carbon cycle in the Arctic to climate change. *Ecol. Monogr.* 79, 523–555. doi: 10.1890/08-2025.1

Meyers, P. A. (1994). Preservation of elemental and isotopic source identification of sedimentary organic matter. *Chem. Geol.* 114, 289–302. doi: 10.1016/0009-2541(94)90059-0

Mudie, P. J., Keen, C. E., Hardy, A., and Viiks, G. (1984). Multivariate analysis and quantitative palcoecology of benthic foraminifera in surface and late Quaternary shelf sediments, northern Canada. *Mar. Micropaleontol.* 8, 283–313. doi: 10.1016/0377-8398(84)90018-5

Murray, J. W. (2006). *Ecology and Applications of Benthic Foraminifera*. Cambridge: Cambridge University Press.

Nelson, D. C., Barker Jørgensen, B., and Revsbech, N. P. (1986). Growth pattern and yield of a chemoautotrophic *Beggiatoa* sp. in oxygen-sulfide microgradients. *Appl. Environ. Microbiol.* 52, 225–233.

Niemann, H., Lösekann, T., de Beer, D., Elvert, M., Nadalig, T., Knittel, K., et al. (2006). Novel microbial communities of the Haakon Mosby mud volcano and their role as a methane sink. *Nature* 443, 854–858. doi: 10.1038/nature05227

Overpeck, J., Hughen, K., Hardy, D., Bradley, R., Case, R., Douglas, M., et al. (1997). Arctic environmental change of the last four centuries. *Science* 278, 1251–1256. doi: 10.1126/science.278.5341.1251

Panieri, G. (2006). Foraminiferal response to an active methane seep environment: a case study from the Adriatic Sea. *Mar. Micropaleontol.* 61, 116–130. doi: 10.1016/j.marmicro.2006.05.008

Panieri, G., and Sen Gupta, B. K. (2008). Benthic foraminifera of the blake ridge hydrate mound, Western North Atlantic Ocean. *Mar. Micropaleontol.* 66, 91–102. doi: 10.1016/j.marmicro.2007.08.002

Panieri, G., Bünz, S., Fornari, D. J., Escartin, J., Serov, P., Jansson, P., et al. (2017). An integrated view of the methane system in the pockmarks at Vestnesa Ridge, 79°N. *Mar. Geol.* 390, 282–300. doi: 10.1016/j.margeo.2017.06.006

Panieri, G., Graves, C. A., and James, R. H. (2016). Paleo-methane emissions recorded in foraminifera near the landward limit of the gas hydrate stability zone off- shore western Svalbard. *Geochem. Geophys. Geosyst.* 17, 521–537. doi: 10.1002/2015GC006153

Panieri, G., James, R. H., Camerlenghi, A., Westbrook, G. K., Consolaro, C., Cacho, I., et al. (2014). Record of methane emissions from the West Svalbard continental margin during the last 23,500 years revealed by δ13C of benthic foraminifera. *Glob. Planet. Change* 122, 151–160. doi: 10.1016/j.gloplacha.2014. 08.014

Petersen, C. J., Bünz, S., Hustoft, S., Mienert, J., and Klaeschen, D. (2010). High-resolution P-Cable 3D seismic imaging of gas chimney structures in gas hydrated sediments of an Arctic sediment drift. *Mar. Petrol. Geol.* 27, 1981–1994. doi: 10.1016/j.marpetgeo.2010.06.006

Plaza-Faverola, A., Bünz, S., Johnson, J. E., Chand, S., Knies, J., Mienert, J., et al. (2015). Role of tectonic stress in seepage evolution along the gas hydrate-charged Vestnesa Ridge. *Fram. Strait Geophys. Res. Lett.* 42, 733–742. doi: 10.1002/2014GL062474

Polyak, L., Korsun, S., Febo, A. L., Stanovoy, V., Khusid, T., Hald, M., et al. (2002). Benthic foraminiferal assemblages from the Southern Kara Sea, a river-influenced Arctic marine environment. *J. Foraminiferal Res.* 32, 252–273. doi: 10.2113/32.3.252

Polyak, L., and Solhelm, A. (1994). Late and postglacial environments in the northern Barents Sea west of Franz Josef Land. *Polar Res.* 13, 197–207. doi: 10.3402/polar.v13i2.6693

Preisler, A., de Beer, D., Lichtschlag, A., Lavik, G., Boetius, A., and Barker Jørgensen, B. (2007). Biological and chemical sulfide oxidation in a Beggiatoa inhabited marine sediment. *ISME J.* 1, 341–353. doi: 10.1038/ismej.2007.50

Rasmussen, T. L., Thomsen, E., Slubowska, M. A., Jessen, S., Solheim, A., and Koc, N. (2007). Paleoceanographic evolution of the SW Svalbard margin (76°N) since 20,000 14C yr BP. *Q. Res.* 67, 100–114. doi: 10.1016/j.yqres.2006.07.002

Rathburn, A. E., Levin, L. A., Held, Z., and Lohmann, K. C. (2000). Benthic foraminifera associated with cold methane seeps on the northern California margin: ecology and stable isotopic composition. *Mar. Micropaleontol.* 38, 247–266. doi: 10.1016/s0377-8398(00)00005-0

Rathburn, A. E., Pereź, M. E., Martin, J. B., Day, S. A., Mahn, C., Gieskes, J., et al. (2003). Relationships between the distribution and stable isotopic composition of living benthic foraminifera and cold methane seep biogeochemistry in Monterey Bay, California. *Geochem. Geophys. Geosyst.* 4:1106. doi: 10.1029/2003GC000595

Ruby, E. G., Jannasch, H. W., and Deuser, W. (1987). Gulf of Mexico hydrocarbon seep communities XI. Carbon isotopic fractionation during fatty acid biosynthesis of seep organisms and its implication for chemosynthetic processes. *Appl. Environ. Microbiol.* 53, 1940–1943.

Sahling, H., Rickert, D., Lee, R. W., Linke, P., and Suess, E. (2002). Macrofaunal community structure and sulfide flux at gas hydrate deposits from the Cascadia convergent margin. NE Pacific. *Mar. Ecol. Prog. Ser.* 231, 121–138. doi: 10.3354/meps231121

Schneider, A., Crémière, A., Panieri, G., Lepland, A., and Knies, J. (2017). Diagenetic alteration of benthic foraminifera from a methane seep site on Vestnesa Ridge (NW Svalbard). *Deep Sea Res. I* 123, 22–34. doi: 10.1016/j.dsr. 2017.03.001

Schneider, A., Panieri, G., Lepland, A., Consolaro, C., Crèmiére, A., Forwick, M., et al. (2018). Arctic seafloor methane seepage since the Last Glacial Maximum. *Q. Sci. Rev.* 193, 98–117. doi: 10.1016/j.quascirev.2018.06.006

Schönfeld, J. (2002). Recent benthic foraminiferal assemblages in deep high-energy environments from the Gulf of Cadiz (Spain). *Mar. Micropaleontol.* 44, 141–162. doi: 10.1016/S0377-8398(01)00039-1

Schönfeld, J., Alve, E., Geslin, E., Jorissen, F., Korsun, S., and Spezzaferri, S. (2012). The FOBIMO (Foraminiferal Bio-Monitoring) initiative—Towards a standardized protocol for soft-bottom benthic foraminiferal monitoring studies. *Mar. Micropaleontol.* 9, 1–13. doi: 10.1016/j.marmicro.2012.06.001

Schulz, H. N. (2006). "The genus Thiomargarita," in *The Prokaryotes*, eds M. Dworkin, S. Falkow, E. Rosenberg, K. H. Schleifer, and E. Stackebrandt, (New York, NY: Springer), 1156–1163. doi: 10.1007/0-387-30746-x_47

Screen, J. A., and Simmonds, I. (2010). The central role of diminishing sea ice in recent Arctic temperature amplification. *Nature* 464, 1334–1337. doi: 10.1038/nature09051

Seidenkrantz, M.-S. (1995). *Cassidulina teretis* Tappan and *Cassidulina neoteretis* new species (Foraminifera): stratigraphic markers for deep sea and outer shelf areas. *J. Micropalaeontol.* 14, 145–157. doi: 10.1144/jm.14.2.145

Seidenkrantz, M.-S. (2013). Benthic foraminifera as palaeo sea-ice indicators in the subarctic realm - examples from the Labrador Sea-Baffin Bay region. *Q. Sci. Rev.* 79, 135–144. doi: 10.1016/j.quascirev.2013.03.014

Sejrup, H. P., and Guibault, J. P. (1980). *Cassidulina reniforme* and *C. obtusa* (foraminifera), taxonomy, distribution and ecology. *Sarsia* 65, 79–85. doi: 10.1080/00364827.1980.10431476

Sen Gupta, B. K., and Aharon, P. (1994). Benthic foraminifera of bathyal hydrocarbon vents of the Gulf of Mexico: initial report on communities and stable isotopes. *Geo Mar. Lett.* 14, 88–96. doi: 10.1007/bf01203719

Sen Gupta, B. K., Platon, E., and Lobegeier, M. K. (2002). "Benthic foraminifera of Gulf of Mexico. Geological Society of Australia, Abstracts No. 68," in *Proceedings of the First International Palaeontological Congress*, Sydney, 142–143.

Sen Gupta, B. K., Platon, E., Bernhard, J. M., and Aharon, P. (1997). Foraminiferal colonization of hydrocarbon-seep bacterial mats and underlying sediment, Gulf of Mexico slope. *J. Foraminiferal Res.* 27, 292–300. doi: 10.2113/gsjfr.27.4.292

Sen Gupta, B. K., Smith, L. E., and Lobegeier, M. K. (2007). Attachment of Foraminifera to vestimentiferan tubeworms at cold seeps: refuge from seafloor hypoxia and sulfide toxicity. *Mar. Micropaleontol.* 62, 1–6. doi: 10.1016/j.marmicro.2006.06.007

Serreze, M. C., and Barry, R. G. (2011). Processes and impacts of Arctic amplification: a research synthesis. *Glob. Planet. Change* 77, 85–96. doi: 10.1016/j.gloplacha.2011.03.004

Sievert, S. M., Wieringa, E. B. A., Wirsen, C. O., and Taylor, C. D. (2007). Growth and mechanism of filamentous-sulfur formation by *Candidatus Arcobacter sulfidicus* in opposing oxygen-sulfide gradients. *Environ. Microbiol.* 9, 271–276. doi: 10.1111/j.1462-2920.2006.01156.x

Smith, A. J., Mienert, J., Bünz, S., and Greinert, J. (2014). Thermogenic methane injection via bubble transport into the upper Arctic Ocean from the hydrate-charged Vestnesa Ridge. *Svalbard. Geochem. Geophys. Geosyst.* 15, 1945–1959. doi: 10.1002/2013GC005179

Sztybor, K., and Rasmussen, T. L. (2017a). Diagenetic disturbances of marine sedimentary records from methane influenced environments in the Fram Strait as indications of variation in seep intensity during the last 35 000 years. *Boreas* 46, 212–228. doi: 10.1111/bor.12202

Sztybor, K., and Rasmussen, T. L. (2017b). Late glacial and deglacial palaeoceanographic changes at Vestnesa Ridge, Fram Strait: methane seep versus non-seep environments. *Palaeogeogr. Palaeoclimatol. Palaeoecol.* 476, 77–89. doi: 10.1016/j.palaeo.2017.04.001

Talwani, M., and Eldholm, O. (1977). Evolution of the Norwegian-Greenland Sea. *Geol. Soc. Am. Bull.* 88, 969–999.

Thiede, J., Winkler, A., Wolf-Welling, T., Eldholm, O., Myhre, A. M., Baumann, K. H., et al. (1998). Late Cenozoic history of the Polar North Atlantic: results from ocean drilling. *Q. Sci. Rev.* 17, 185–208. doi: 10.1016/s0277-3791(97)00076-0

Torres, M. E., McManus, J., Hammond, D. E., de Angelis, M. A., Heeschen, K. U., Colbert, S. L., et al. (2002). Fluid and chemical fluxes in and out of sediments

hosting methane hydrate deposits on Hydrate Ridge, OR, I: hydrological provinces. *Earth Planet. Sci. Lett.* 201, 525–540. doi: 10.1016/s0012-821x(02)00733-1

Torres, M. E., Mix, A. C., Kinports, K., Haley, B., Klinkhammer, G. P., McManus, J., et al. (2003). Is methane venting at the seafloor recorded by δ^{13}C of benthic foraminifera shells? *Paleoceanography* 18:1062. doi: 10.1029/2002PA000824

Treude, T., Boetius, A., Knittel, K., Wallmann, K., and Barker Jørgensen, B. (2003). Anaerobic oxidation of methane above gas hydrates at Hydrate Ridge, NE Pacific Ocean. *Mar. Ecol. Progr. Ser.* 264, 1–14. doi: 10.3354/meps264001

Vogt, P. R., Crane, K., Sundvor, E., Max, M. D., and Pfirman, S. L. (1994). Methane-generated (?) pockmarks on young, thickly sedimented oceanic crust in the Arctic: Vestnesa Ridge. *Fram Strait. Geol.* 22, 255–258.

Walton, W. R. (1952). Techniques for recognition of living foraminifera. contribution of the Cushman. *Found. Foram. Res.* 3, 56–60.

Whiticar, M. J. (1999). Carbon and hydrogen isotope systematics of bacterial formation and oxidation of methane. *Chem. Geol.* 161, 291–314. doi: 10.1016/s0009-2541(99)00092-3

Wollenburg, J. E., and Kuhnt, W. (2000). The response of benthic foraminifera to carbon flux and primary production in the Arctic Ocean. *Mar. Micropaleontol.* 40, 189–231. doi: 10.1016/s0377-8398(00)00039-6

Wollenburg, J. E., and Mackensen, A. (1998). Living benthic foraminifers from the central Arctic Ocean: faunal composition, standing stock and diversity. *Mar. Micropaleontol.* 34, 153–185. doi: 10.1016/s0377-8398(98)00007-3

Wollenburg, J. E., and Mackensen, A. (2009). The ecology and distribution of benthic foraminifera at the Håkon Mosby mud volcano (SW Barents Sea slope). *Deep Sea Res. I* 56, 1336–1370. doi: 10.1016/j.dsr.2009.02.004

Wollenburg, J. E., Knies, J., and Mackensen, A. (2004). High-resolution paleoproductivity fluctuations during the past 24 kyr as indicated by benthic foraminifera in the marginal Arctic Ocean. *Palaeogeogr. Palaeoclimatol. Palaeoecol.* 204, 209–238. doi: 10.1016/s0031-0182(03)00726-0

Wollenburg, J. E., Kuhnt, W., and Mackensen, A. (2001). Changes in Arctic Ocean paleoproductivity and hydrography during the last 145 kyr: the benthic foraminiferal record. *Paleoceanography* 16, 65–77. doi: 10.1029/1999pa000454

Yao, H., Hong, W.-L., Panieri, G., Sauer, S., Torres, M. E., Lehmann, M. F., et al. (2019). Fracture-controlled fluid transport supports microbial methane-oxidizing communities at Vestnesa Ridge. *Biogeosciences* 16, 2221–2232. doi: 10.5194/bg-16-2221-2019